

Vehicle Positioning with Map Matching Using Integration of a Dead Reckoning System and GPS

Examensarbete utfört i Reglerteknik
vid Tekniska Högskolan i Linköping
av

David Andersson
Johan Fjellström

Reg nr: LiTH-ISY-EX-3457-2004
Linköping 2004

Vehicle Positioning with Map Matching Using Integration of a Dead Reckoning System and GPS

Examensarbete utfört i Reglerteknik
vid Tekniska Högskolan i Linköping
av


**David Andersson
Johan Fjellström**

Reg nr: LiTH-ISY-EX-3457-2004

Supervisor: **Hans Andersson
Martin Enqvist**

Examiner: **Svante Gunnarsson**

Linköping 26th February 2004.

 LINKÖPINGS UNIVERSITET	Avdelning, Institution Division, Department Institutionen för systemteknik 581 83 LINKÖPING	Datum Date 2004-02-13								
Språk Language Svenska/Swedish X Engelska/English	Rapporttyp Report category Licentiatavhandling X Examensarbete C-uppsats D-uppsats Övrig rapport _____	<table border="1"> <tr> <td colspan="2">ISBN</td> </tr> <tr> <td>ISRN</td> <td>LITH-isy-ex-3457-2004</td> </tr> <tr> <td>Serietitel och serienummer</td> <td>ISSN</td> </tr> <tr> <td>Title of series, numbering</td> <td>_____</td> </tr> </table>	ISBN		ISRN	LITH-isy-ex-3457-2004	Serietitel och serienummer	ISSN	Title of series, numbering	_____
ISBN										
ISRN	LITH-isy-ex-3457-2004									
Serietitel och serienummer	ISSN									
Title of series, numbering	_____									
URL för elektronisk version http://www.ep.liu.se/exjobb/isy/2004/3457/										
<table border="1"> <tr> <td>Titel</td> <td>Integration av dödräkning och GPS för fordonspositionering med map matching</td> </tr> <tr> <td>Title</td> <td>Vehicle Positioning with Map Matching Using Integration of a Dead Reckoning System and GPS</td> </tr> <tr> <td>Författare</td> <td>David Andersson, Johan Fjellström</td> </tr> <tr> <td>Author</td> <td></td> </tr> </table>			Titel	Integration av dödräkning och GPS för fordonspositionering med map matching	Title	Vehicle Positioning with Map Matching Using Integration of a Dead Reckoning System and GPS	Författare	David Andersson, Johan Fjellström	Author	
Titel	Integration av dödräkning och GPS för fordonspositionering med map matching									
Title	Vehicle Positioning with Map Matching Using Integration of a Dead Reckoning System and GPS									
Författare	David Andersson, Johan Fjellström									
Author										
<table border="1"> <tr> <td>Sammanfattning</td> </tr> <tr> <td>Abstract</td> </tr> <tr> <td> <p>To make driving easier and safer, modern vehicles are equipped with driver support systems. Some of these systems, for example navigation or curvature warning systems, need the global position of the vehicle. To determine this position, the Global Positioning System (GPS) or a Dead Reckoning (DR) system can be used. However, these systems have often certain drawbacks. For example, DR systems suffer from error growth with time and GPS signal masking can occur. By integrating the DR position and the GPS position, the complementary characteristics of these two systems can be used advantageously.</p> <p>In this thesis, low cost in-vehicle sensors (gyroscope and speedometer) are used to perform DR and the GPS receiver used has a low update frequency. The two systems are integrated with an extended Kalman filter in order to estimate a position. The evaluation of the implemented positioning algorithm shows that the system is able to give an estimated position in the horizontal plane with a relatively high update frequency and with the accuracy of the GPS receiver used. Furthermore, it is shown that the system can handle GPS signal masking for a period of time.</p> <p>In order to increase the performance of a positioning system, map matching can be added. The idea with map matching is to compare the estimated trajectory of a vehicle with roads stored in a map data base, and the best match is chosen as the position of the vehicle. In this thesis, a simple off-line map matching algorithm is implemented and added to the positioning system. The evaluation shows that the algorithm is able to distinguish roads with different direction of travel from each other and handle off-road driving.</p> </td> </tr> </table>			Sammanfattning	Abstract	<p>To make driving easier and safer, modern vehicles are equipped with driver support systems. Some of these systems, for example navigation or curvature warning systems, need the global position of the vehicle. To determine this position, the Global Positioning System (GPS) or a Dead Reckoning (DR) system can be used. However, these systems have often certain drawbacks. For example, DR systems suffer from error growth with time and GPS signal masking can occur. By integrating the DR position and the GPS position, the complementary characteristics of these two systems can be used advantageously.</p> <p>In this thesis, low cost in-vehicle sensors (gyroscope and speedometer) are used to perform DR and the GPS receiver used has a low update frequency. The two systems are integrated with an extended Kalman filter in order to estimate a position. The evaluation of the implemented positioning algorithm shows that the system is able to give an estimated position in the horizontal plane with a relatively high update frequency and with the accuracy of the GPS receiver used. Furthermore, it is shown that the system can handle GPS signal masking for a period of time.</p> <p>In order to increase the performance of a positioning system, map matching can be added. The idea with map matching is to compare the estimated trajectory of a vehicle with roads stored in a map data base, and the best match is chosen as the position of the vehicle. In this thesis, a simple off-line map matching algorithm is implemented and added to the positioning system. The evaluation shows that the algorithm is able to distinguish roads with different direction of travel from each other and handle off-road driving.</p>					
Sammanfattning										
Abstract										
<p>To make driving easier and safer, modern vehicles are equipped with driver support systems. Some of these systems, for example navigation or curvature warning systems, need the global position of the vehicle. To determine this position, the Global Positioning System (GPS) or a Dead Reckoning (DR) system can be used. However, these systems have often certain drawbacks. For example, DR systems suffer from error growth with time and GPS signal masking can occur. By integrating the DR position and the GPS position, the complementary characteristics of these two systems can be used advantageously.</p> <p>In this thesis, low cost in-vehicle sensors (gyroscope and speedometer) are used to perform DR and the GPS receiver used has a low update frequency. The two systems are integrated with an extended Kalman filter in order to estimate a position. The evaluation of the implemented positioning algorithm shows that the system is able to give an estimated position in the horizontal plane with a relatively high update frequency and with the accuracy of the GPS receiver used. Furthermore, it is shown that the system can handle GPS signal masking for a period of time.</p> <p>In order to increase the performance of a positioning system, map matching can be added. The idea with map matching is to compare the estimated trajectory of a vehicle with roads stored in a map data base, and the best match is chosen as the position of the vehicle. In this thesis, a simple off-line map matching algorithm is implemented and added to the positioning system. The evaluation shows that the algorithm is able to distinguish roads with different direction of travel from each other and handle off-road driving.</p>										
<table border="1"> <tr> <td>Nyckelord</td> </tr> <tr> <td>Keyword</td> </tr> <tr> <td>Vehicle Positioning, Dead Reckoning, GPS, Extended Kalman Filter, Map Matching</td> </tr> </table>			Nyckelord	Keyword	Vehicle Positioning, Dead Reckoning, GPS, Extended Kalman Filter, Map Matching					
Nyckelord										
Keyword										
Vehicle Positioning, Dead Reckoning, GPS, Extended Kalman Filter, Map Matching										

Abstract

To make driving easier and safer, modern vehicles are equipped with driver support systems. Some of these systems, for example navigation or curvature warning systems, need the global position of the vehicle. To determine this position, the Global Positioning System (GPS) or a Dead Reckoning (DR) system can be used. However, these systems have often certain drawbacks. For example, DR systems suffer from error growth with time and GPS signal masking can occur. By integrating the DR position and the GPS position, the complementary characteristics of these two systems can be used advantageously.

In this thesis, low cost in-vehicle sensors (gyroscope and speedometer) are used to perform DR and the GPS receiver used has a low update frequency. The two systems are integrated with an extended Kalman filter in order to estimate a position. The evaluation of the implemented positioning algorithm shows that the system is able to give an estimated position in the horizontal plane with a relatively high update frequency and with the accuracy of the GPS receiver used. Furthermore, it is shown that the system can handle GPS signal masking for a period of time.

In order to increase the performance of a positioning system, map matching can be added. The idea with map matching is to compare the estimated trajectory of a vehicle with roads stored in a map data base, and the best match is chosen as the position of the vehicle. In this thesis, a simple off-line map matching algorithm is implemented and added to the positioning system. The evaluation shows that the algorithm is able to distinguish roads with different direction of travel from each other and handle off-road driving.

Keywords: Vehicle Positioning, Dead Reckoning, GPS, Extended Kalman Filter, Map Matching

Acknowledgments

First of all we would like to thank our supervisor PhD Student Martin Enqvist, Linköping Institute of Technology, for all his help with this thesis. Martin has always had time for our questions and his comments on this thesis have been very valuable. We are also grateful to our supervisor Hans Andersson, Volvo Technology Corporation, for interesting discussions and his help with practical arrangements. We would also like to thank our examiner Professor Svante Gunnarsson, Linköping Institute of Technology. Special thanks to Andreas Ekfjorden for technical assistance and to Erik Johnson for his help with L^AT_EX. Finally, we would like to thank the staff at the Department of Human System Integration for making our time there a great time.

Gothenburg, January 2004

David Andersson & Johan Fjellström

Notation

Notational conventions used in this thesis are presented in this chapter.

Symbols

δx	Error state vector
$\Delta_{\dot{\Psi}}$	Yaw rate offset
$\Delta_{\dot{\Theta}}$	Pitch rate offset
$\dot{\Psi}$	Yaw rate
$\dot{\Theta}$	Pitch rate
\hat{x}	Estimated state vector
λ	Longitude
ϕ	Latitude
Ψ	Yaw angle
Θ	Pitch angle
\tilde{x}	State estimation error
C	Map matching tuning parameter
d	Geodetic height
e	Measurement noise
E	East coordinate
F	Linear system matrix
G	Process noise matrix
H	Linear measurement matrix
K	Kalman gain matrix
N	North coordinate
P	Covariance matrix of the state estimation error
Pos	Position
Q	Covariance matrix of the process noise

R	Covariance matrix of the measurement noise
r	Distance from a point to the mass centre of the earth
S	Speed scale error
T	Sample time
t	Time delay
v	Speed
w	Process noise
x	State vector
x^{nom}	Nominal state vector
y	System output
Z	Height coordinate

Operators and functions

σ	Standard deviation
E	Expected value
f	System functions
h	Measurement functions

Abbreviations

2D	Two dimensional
3D	Three dimensional
CAN	Controller Area Network
CM	Mass Centre of the earth
DOP	Dilution Of Precision
DR	Dead Reckoning
ECEF	Earth Centered Earth Fixed
EKF	Extended Kalman Filter
GPS	Global Positioning System
INS	Inertial Navigation System
km	Kilometre
m	Metre
NEZ	North East Height
U.S. DoD	United States Department of Defence
UTM	Universal Transverse Mercator
WGS-84	World Geodetic System 1984
VTEC	Volvo TEChnology

Contents

Abstract	i
1 Introduction	1
1.1 Background	1
1.2 Volvo Technology Corporation	2
1.3 Problem statement and objectives	2
1.4 Limitations	3
1.5 Thesis outline	3
2 Coordinates and Maps	5
2.1 Earth models	5
2.2 Coordinate frames	5
2.3 Cartesian, geocentric and geodetic coordinates	6
2.4 Map projections	8
3 Positioning Techniques	11
3.1 Dead reckoning	11
3.2 In-vehicle sensors	12
3.2.1 Gyroscopes	13
3.2.2 Speedometers	13
3.3 GPS	14
3.4 Integration of DR and GPS	15
3.5 Map matching	16
3.5.1 Semi-deterministic algorithms	17
3.5.2 Probabilistic algorithms	18
4 State Estimation Theory	21
4.1 State space description	21
4.2 Observers	22
4.3 Kalman filtering	22
4.4 Linearised Kalman filters	23
4.5 Extended Kalman filters	24

5	Measurements and Data Acquisition	27
5.1	Data acquisition	27
5.2	GPS measurements	28
5.3	In-vehicle sensor measurements	29
5.4	Limitations due to data errors	29
5.5	DR and GPS trajectories	29
6	Positioning System with Complete Vehicle State Model	31
6.1	Complete vehicle state model	31
6.1.1	Gyroscope error model	31
6.1.2	Speedometer error model	32
6.1.3	GPS error model	32
6.1.4	Complete vehicle state equations	33
6.2	Implementation of the complete vehicle state model	33
6.3	Real-time implementation of the complete vehicle state model	37
6.4	Limitations of positioning system with vehicle state model	37
6.5	Evaluation of positioning system with vehicle state model	37
6.5.1	Absolute position	38
6.5.2	Yaw rate and pitch rate estimation	39
6.5.3	Gyroscope offset estimation	41
6.5.4	Attitude estimation	43
6.5.5	GPS signal masking	44
7	Positioning System with Error State Model	47
7.1	Error state equations	47
7.2	Implementation of the error state model	48
7.3	Evaluation of positioning system with error state model	50
8	Map Matching	53
8.1	Map data base	53
8.2	Implementation of a probabilistic point-to-point and heading map matching algorithm	53
8.3	Evaluation of the map matching algorithm	54
9	Conclusions	57
9.1	Results	57
9.2	Future work	58
	Bibliography	59
A	System Matrices	61
A.1	System matrices for the complete vehicle state model	61
A.2	Design matrices for the complete vehicle state model	63
A.3	System matrices for the error state model	63
A.4	Design parameters for the error state model	64

B	Transformations	67
B.1	Transformation between WGS-84 and UTM coordinates	67
B.2	Transformation between UTM and WGS-84 coordinates	68

Chapter 1

Introduction

The performances of some driver support systems are depending on the accuracy of which the global position of the vehicle can be determined. Volvo Technology Corporation (VTEC) is a company that has driver support system development as one business area and is therefore in need of a positioning system. In this master thesis project, with VTEC as client, a real-time positioning system, using dead reckoning (DR) and the Global Positioning System (GPS), is developed. The background, problem statement, objectives and limitations are given in this chapter.

1.1 Background

In modern vehicles, driver support systems are getting more and more common. These systems are often designed to make driving easier and safer. This can be done either by providing the driver with useful information or by implementing active support systems. In some driver support systems, for example navigation systems, the global (or absolute) position of the vehicle is of great concern. The problem of determining the vehicle's global coordinates in a known coordinate system is called positioning. Positioning can be done, for example, using a GPS, a DR system or a combination of these two. A DR system uses information such as starting position, speed and driving directions to calculate the vehicle's position. Systems using only DR often have accuracy problems since the errors often grow with time. GPS, on the other hand, suffers from problems with signal masking in some areas, such as urban canyon areas and in tunnels. Integration of these systems is one way to avoid the problems occurring when the systems are used separately. Positioning systems, like the ones mentioned, are available on the market at different prices and with different accuracy.

Another positioning technique, besides the ones mentioned above, is map matching. The main idea in this approach is that the vehicle's trajectory is compared, or matched, to a digital map and that the point which gives the best match is chosen

as the position estimate. By adding map matching to a positioning system, the accuracy of the positioning system can be increased. Digital maps are also needed for some driver support systems like curvature warning systems. Just like positioning systems, digital maps are available on the market. However, many of these digital maps contain information about road intersections, but not the curvature information needed for a curvature warning system. The detailed maps that are available are often very expensive.

1.2 Volvo Technology Corporation

This master thesis project has been performed at the Department of Human System Integration at Volvo Technology Corporation (VTEC) in Gothenburg. VTEC has about 300 employees and is located at Lundbystrand and Chalmers Science Park in Gothenburg and at Volvo's establishments in Lyon, France and in Greensboro, USA. VTEC is an innovation company with Volvo Cars and Volvo Group Business Areas & Units as primary customers. All development at VTEC is done on contract basis and the main research and development areas are transportation, telematics, internet applications, databases, ergonomics, electronics, combustion, mechanics, industrial hygiene and industrial processes. Human System Integration is a department working in the following areas: driver awareness, virtual reality and driving simulation, user impression and satisfaction, driver support systems and interaction design. More information about VTEC can be found in [11].

1.3 Problem statement and objectives

VTEC is interested in having their own positioning system for determining a vehicle's position and for creating digital maps with desirable information. The positioning system should estimate the position using a self adjusting, with respect to GPS data, Kalman filter, with DR position and GPS data as inputs. The DR system, providing the DR position, should have the vehicle speed and the angular velocities as inputs. The sample frequency of the positioning system should be at least 20 Hz and the system should be able to handle GPS signal masking. The system should be compatible with the interface in Volvo cars and trucks. Map matching should also be added to the system and used in order to improve the position estimates as soon as a digital map has been created with the initial positioning system.

The objectives with this thesis are to use DR and GPS in order to estimate the position of a driving vehicle with a Kalman filter and to match the estimated position against a digital map.

1.4 Limitations

The positioning system only has to perform well in the geographic area of Sweden and another limitation is that the positioning system only needs to be compatible with Volvo cars and trucks with a Controller Area Network (CAN) bus. Furthermore, the system only has to handle GPS signal masking for a limited time during run time and that GPS data have to be available at the time the system is started. The positioning solution including map matching is allowed to be an off-line solution.

1.5 Thesis outline

The theory on earth models, coordinate frames and map projections are described in Chapter 2. In Chapter 3, a review of positioning techniques and an approach to integrate two of these techniques are given. This chapter also gives an introduction to map matching algorithms and in-vehicle sensors. Chapter 4 describes the state estimation theory and in Chapter 5, the measurement and data acquisition is reviewed. A vehicle positioning system using integration of DR and GPS is presented and evaluated in Chapter 6. An alternative integration approach is described in Chapter 7. A map matching algorithm and the evaluation of it is given in Chapter 8. Finally, a summary of the results and some ideas for future work are presented in Chapter 9.

Chapter 2

Coordinates and Maps

The output of a positioning system is always a set of coordinates. Of course, in order to specify a position as a number of coordinates, a coordinate system is needed. Often positioning systems also need earth models and two-dimensional (2D) projections of the earth for proper functionality. This chapter will give the fundamentals of earth models, coordinate system and projections.

2.1 Earth models

The surface of the earth is often used as a reference in positioning and navigation systems and for this purpose a model of the earth is needed [2]. The most simple earth model is a sphere with a fixed axis of rotation. The World Geodetic System 1984 (WGS-84) earth model, developed by the United States Department of Defence (U.S. DoD), is a more advanced model, where the mean sea level is approximated by an ellipsoid. The axis of rotation is the rotation axis of the earth and the centre of the ellipsoid is at the mass centre of the earth. The polar radius is modelled as approximately 6357 km and the equatorial radius is modelled as 6378 km. The WGS-84 earth model is an international standard for navigation coordinates [7].

2.2 Coordinate frames

The location of a point can be specified using a vector from an origin to the point itself and to do this, a coordinate system is needed. Some coordinate frames that are of interest when designing a positioning system are listed below:

- **Inertial frame:** A coordinate frame with origin in the centre of earth. The X- and Y-axes lie in the equatorial plane and the Z-axis points at the north pole. The inertial frame is fixed relative the fixed stars. In navigation applications concerning navigation on earth, this coordinate frame can be considered an inertial system.

- **ECEF frame:** An earth-centred, earth-fixed coordinate frame. This coordinate frame is similar to the Inertial frame but rotates with the earth and has the X-axis towards the Greenwich meridian. Two different types of coordinates are common for describing the location of the point in the ECEF frame, namely three-dimensional (3D) Cartesian coordinates and geodetic coordinates. Different coordinates will be discussed further in Section 2.3.
- **WGS-84 frame:** An earth-centred, earth fixed frame. This coordinate frame uses geodetic coordinates and the WGS-84 ellipsoidal earth model. The WGS-84 frame has its prime meridian through Greenwich and is an example of an ECEF frame.
- **NEZ frame:** A coordinate frame with its origin in the vehicle (mass centre of the vehicle or centre of sensor cluster) and where the N-axis always points north, E-axis always points east and Z-axis points up from the centre of the earth.
- **Body frame:** A coordinate frame with the same origin as the NEZ coordinate frame. The X-axis is in the direction of the car, the Z-axis is through the roof of the vehicle and the Y-axis completes the right hand orthogonal coordinate frame.

More information on coordinate frames can be found in [2, 4, 15].

2.3 Cartesian, geocentric and geodetic coordinates

As mentioned in Section 2.2, 3D Cartesian (normally written X, Y and Z) and geodetic coordinates are two alternative types of coordinates used in positioning applications. A third additional type of coordinate system is the geocentric coordinate system, see Figure 2.1. Geocentric coordinates use a coordinate frame with origin at the mass centre of the earth and define the coordinates of a point with latitude (ϕ), longitude (λ) and distance from the origin to the point itself (r) [15].

A geodetic coordinate system consists of an ellipsoid (for example the WGS-84 earth model), the equatorial plane of the ellipsoid and a plane through the polar axis of the ellipsoid [15]. A geodetic coordinate system and a 3D Cartesian coordinate system are visualised in Figure 2.2. The geodetic latitude (ϕ) is the angle between the equatorial plane and the extension of the normal to the ellipsoid surface towards the interior of the earth. Note that the extension of the normal to the ellipsoidal earth model towards the interior of the earth in general will not intersect with the centre of earth due to the elliptic form of the earth model. The geodetic longitude (λ) is the angle in the equatorial plane between the prime meridian and the orthogonal projection of the point of interest in the equatorial plane. The geodetic height (d) is the distance between the point of interest and the ellipsoid, measured along the normal to the surface of the ellipsoid [15]. The geodetic height

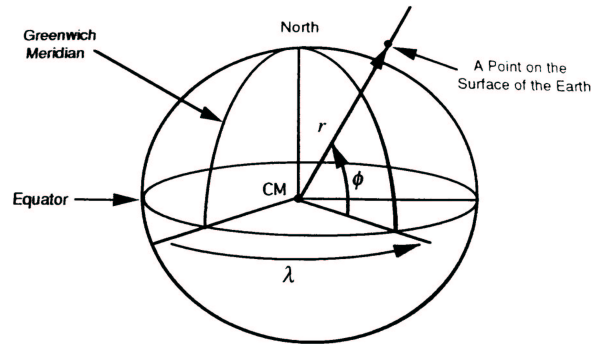


Figure 2.1. A geocentric coordinate system with latitude (ϕ), longitude (λ) and the distance from the origin to the point itself (r). CM is the mass centre of the earth [15].

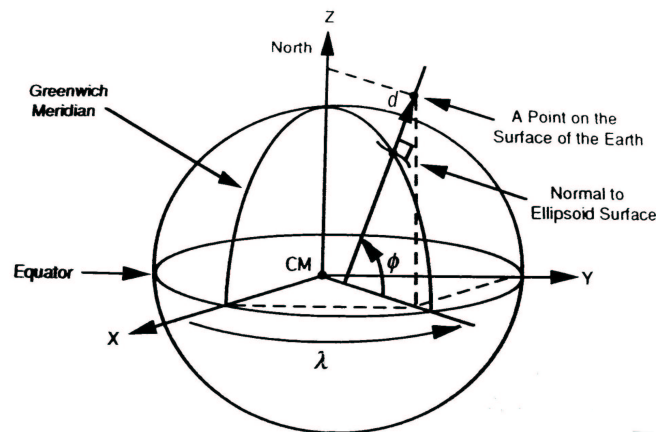


Figure 2.2. A geodetic coordinate system, with latitude (ϕ), longitude (λ) and the geodetic height (d) and a Cartesian coordinate systems with coordinates X, Y and Z. The mass centre of the earth is abbreviated with CM [15].

is an approximation of the height over the sea level, due to the fact that the ellipsoid surface is an approximation of the sea level. The geodetic height should therefore be handled with care, especially in air navigation where height over the surface of the earth is critical.

3D Cartesian coordinates are not very convenient for positioning and navigation, for example moving northeast a certain distance, except at the North pole, will not result in an identical increase in the Z value. Geodetic coordinates are therefore used much more often. However, some problems occur also when geodetic coordinates are used in positioning systems. Although there are mathematical formulas

for calculating a distance from geodetic coordinates and vice versa, these formulas are not as straightforward to use as the corresponding formulas for 2D Cartesian coordinates. In order to avoid this problem, the geodetic latitude and longitude coordinates are often transformed to 2D Cartesian coordinates [15]. This transformation can be performed in several ways using different types of 2D projections called map projections. When referring to a map in this thesis, a 2D map is always considered, if nothing else is specified. A wide variety of projections are available in the literature and some of these will be discussed in the next section.

2.4 Map projections

In general, there are two main types of map projections, namely conformal and equivalent projections. A conformal projection preserves all angles, i.e. the angles on the map are equal to the angles on the surface of the earth. On the other hand, an equivalent projection has a constant ratio between any area on the map and the corresponding area on earth. No projection can be both conformal and equivalent [15]. It is important to note that when a map projection is used to transform one type of coordinates to another, this projection is exact. On the other hand, any 2D representation of the 3D spherical earth is an approximation, no matter which type of projection that is used.

Hence, the use of a 2D projection of the earth, will lead to that an approximation is done. However, this approximation is negligible for daily life map users. As mentioned above, a variety of projections are available and many of these have been developed to approximate a certain local area as good as possible. Unfortunately, the use of these projections on other areas than those the projections are developed for, will often lead to poor or even invalid projections. Therefore, these projections are not very useful for worldwide applications. A projection that has been designed to be used worldwide is the conformal Universal Transverse Mercator (UTM) projection. The UTM projection transforms geodetic coordinates expressed in the WGS-84 frame to 2D UTM coordinates. Transforming WGS-84 coordinates to UTM coordinates is desirable when a GPS is supposed to be integrated with a DR system, which often is carried out directly in UTM coordinates.

The conformal UTM projection partitions the surface of the ellipsoidal earth model into 60 zones, each 6° wide in longitude. Each zone has its own central meridian in the centre of the zone and the zones reach from 80° S to 84° N. The UTM coordinates are 2D Cartesian coordinates with the N axis defined in the north direction and the E axis defined in the east direction. The UTM coordinates are referred to as northing and easting and are given in metres [15]. The origin of each zone is the point where the central meridian intersects the equator. If the origin of each zone would be assigned with a value of 0, all points west of the central meridian in the zone either have to be given negative values or assigned with a direction, for example west of the central meridian. To avoid this, and to give positive values

to all points in a zone, the central meridian in each zone is given a “false” easting of 500 000 m. This implies that the points west of the central meridian will have values lower than 500 000. Similarly, if the equator would be given the northing value 0, all points in the southern hemisphere have to be negative or assigned with a south direction. Therefore the equator is given a “false” northing of 10 000 000 m when referring to a position on the southern hemisphere and 0 when referring to a position on the northern hemisphere [9]. The UTM projection is a worldwide projection and is easy to use for a positioning system design working in one zone. Unfortunately, transitions between different zones are more difficult to handle. Mathematical expressions for the transformations between coordinates expressed in the WGS-84 frame and UTM coordinates can be found in Appendix B.1.

Chapter 3

Positioning Techniques

Today there are three main approaches to vehicle positioning, namely stand-alone, satellite based and terrestrial radio based. Dead reckoning (DR) is one example of a stand-alone approach and can be combined with, for example the Global Positioning System (GPS), which is a satellite based positioning system. In order to perform DR, the speed and direction of travel are needed and these properties can be measured indirectly with in-vehicle sensors. Map matching can be used in order to make the positioning system even more accurate. In this chapter, in-vehicle sensors, DR systems, GPS and map matching will be discussed further.

3.1 Dead reckoning

A DR system uses the fact that it is possible to calculate a vehicle's position at any instance if the starting location and all previous displacements are known. This type of system computes the distance travelled and the direction of travel. A common DR system is the Inertial Navigation System (INS) which calculates the position of the vehicle from its acceleration and angular velocities. Another DR approach is to use the speed (v) and the angular velocities (yaw rate ($\dot{\Psi}$) and pitch rate ($\dot{\Theta}$)) to calculate the vehicle's position and attitude¹. Speed, yaw rate, pitch rate and attitude are all supposed to be constant during a sample period. The equations that can be used to calculate the position and attitude of the vehicle

¹The attitude is the relation between the body frame and the NEZ frame and can be described with three angles, namely the yaw angle, the pitch angle and the roll angle [14]. In this thesis only the yaw angle and the pitch angle are referred to as the attitude.

with this approach are

$$N(k+1) = N(k) + v(k)T \cos(\Theta(k)) \cos(\Psi(k)) \quad (3.1)$$

$$E(k+1) = E(k) + v(k)T \cos(\Theta(k)) \sin(\Psi(k)) \quad (3.2)$$

$$Z(k+1) = Z(k) + v(k)T \sin(\Theta(k)) \quad (3.3)$$

$$\Psi(k+1) = \Psi(k) + T\dot{\Psi}(k) \quad (3.4)$$

$$\Theta(k+1) = \Theta(k) + T\dot{\Theta}(k) \quad (3.5)$$

where T is the sample time and N , E and Z are the north, east and height position coordinates. Ψ is the yaw angle, Θ is the pitch angle and they are in this thesis defined as in Figure 3.1. The expressions (3.1)-(3.5) define the DR approach used

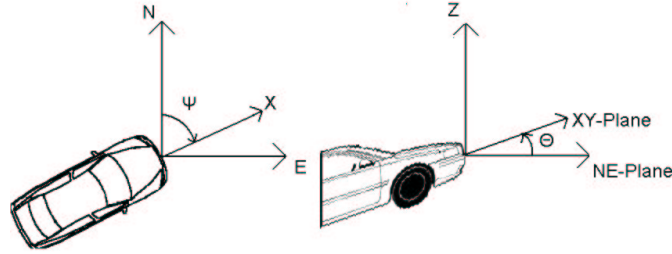


Figure 3.1. The definition of the yaw angle (Ψ) and the pitch angle (Θ) used in this thesis.

in this thesis. Sensor inaccuracies and the assumption of constant speed, yaw rate, pitch rate and attitude over a sample period will lead to errors in position and attitude. These errors tend to accumulate as the vehicle continues to travel and the calculated position and attitude will thus be less accurate over time. An advantage with DR systems, is that they are possible to run with a high sample frequency.

3.2 In-vehicle sensors

Since speed, yaw rate and pitch rate are needed to perform the DR approach described by (3.1)-(3.5), these signals need to be measured. In-vehicles sensors like gyroscopes and speedometers can be used for this purpose.

3.2.1 Gyroscopes

Rate-sensing gyroscopes measure the angular velocities of the vehicle. There are gyroscopes of various types, e.g. mechanical, optical, pneumatic and vibration devices. The most common gyroscope in vehicle positioning systems is of the vibration type. These gyroscopes measure the Coriolis accelerations to determine the angular velocities [15].

The performance of a gyroscope depends on several factors. The most common gyroscopic errors are bias, scale factor error, nonlinearity, scale factor sign asymmetry, dead zone, quantisation error, measurement noise and sensor misalignment [7]. Six of these errors are illustrated in Figure 3.2. For example, as can be seen in the figure, the bias, or the offset, is any nonzero gyroscopic output when the input is zero.

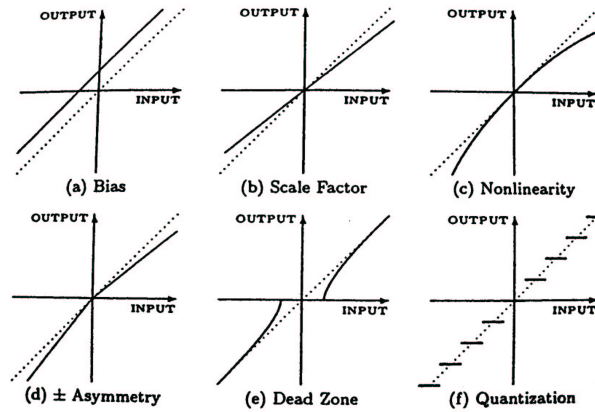


Figure 3.2. An illustration of six common errors in gyroscopes, where the gyroscopic output (solid) is compared with the true output (dashed) [7].

3.2.2 Speedometers

A car speedometer consists of a toothed ferrous wheel attached to the vehicle's wheel and a Hall-effect sensor. This sensor senses each tooth that passes through it. From the fact that the number of degrees between two teeth on the ferrous wheel is known, the rotational velocity of the wheel can be calculated by measuring the time it takes for two teeth to pass the Hall-effect sensor. Under the assumption that the radius of the vehicle's wheel has a nominal value, the speed of the vehicle can be calculated. To get a better approximation of the speed two speedometers are used, one on each of the nondriven wheels [15]. The performance of the speedometer depends mostly on the uncertainty in radius of the vehicle's wheel, but also measurement noise and quantization effects give rise to errors.

3.3 GPS

The GPS is a satellite-based radio navigation system, designed by the U.S. DoD, but accessible also to civilians. The GPS satellite constellation consists of 24 satellites arranged in six orbital planes. Each satellite carries a high precision atomic clock and broadcasts messages at regular and known time instants. Each message includes an identity number and the location of the satellite. A receiver on the ground decodes the message and uses the signal propagation time to calculate a pseudorange. In order to determine its position, the receiver needs to know both the pseudoranges to some of the satellites as well as their positions. Simultaneous observation of at least four satellites permits determination of the 3D coordinates of the receiver. The coordinates can be computed in, for example, an ECEF frame or in a WGS-84 frame [15].

The accuracy of a GPS system is affected by errors in the measurements of the distances from the satellites to the receiver. These errors are commonly referred to as range errors and they include satellite clock, receiver clock, satellite orbit, multipath and atmospheric errors. The accuracy of the position also depends on the geometry of the visible satellites. This is illustrated by a simple example below.

For simplicity, only two satellites for 2D position calculation are considered here, see Figure 3.3. The figure shows four satellites and their pseudorange intervals, and the intersection of two pseudorange intervals (shadowed areas),

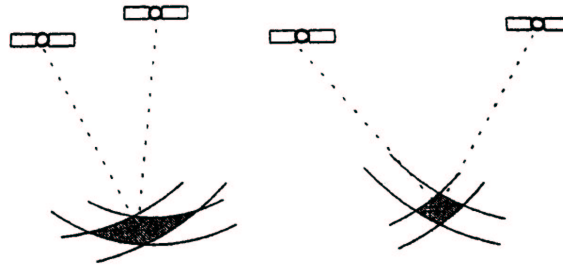


Figure 3.3. Four GPS satellites, their pseudorange intervals (solid) and the intersection of two pseudorange intervals (shadowed areas) [2].

which are the pseudorange plus/minus the range error. In this example, the range errors are supposed to be the same for all four satellites. The position of the receiver is computed based on the data within the shadowed region, which is constructed as the intersection of the pseudorange intervals of two satellites. The geometry to the left has a larger shadowed area, i.e. larger error in the computed position than the geometry to the right and is therefore said to have larger dilution of precision (DOP) [13].

The performance of GPS receivers under heavy foliage and in urban canyon ar-

eas can be poor. Under these circumstances, the GPS receivers will sometimes not be able to observe four or more satellites and the user will hence experience signal masking [8]. Most GPS receivers have a relatively long sample period, approximately 1 s. When the position from the GPS receiver is presented for the user, it can be delayed, sometimes as much as one sample period.

3.4 Integration of DR and GPS

DR systems are possible to run with high sample frequency but suffer from error growth. In contrast, GPS receivers do not suffer from error growth but most common GPS receivers often have low sample frequency [14]. Another drawback with GPS receivers is the risk for signal masking, which never occurs for a DR system. These complementary characteristics indicate that integration of the two systems might be advantageous [4]. This integration can, for example, be done using a Kalman filter. Some theory about Kalman filtering can be found in Chapter 4. Several approaches to Kalman filtering of GPS and DR signals can be found in literature and four of these are described here:

- **Loosely coupled integration with a complete vehicle state model:** The Kalman filter states are the parameters describing the movement of the vehicle in an arbitrary coordinate system. The GPS data and data from in-vehicle sensors are used as measurements [3]. This approach will result in an extended Kalman filter (EKF).
- **Loosely coupled integration with an error state model:** The Kalman filter states are the errors in the GPS and the DR system. The Kalman filter estimate of the position error is used to correct the DR position. The differences between the GPS position and the DR position are used as measurements [14]. This approach can be viewed as if a linearised Kalman filter is used instead of an EKF in the complete vehicle state model approach, with the distinction that the states are position errors.
- **Loosely coupled integration with an error state model and feedback:** This approach uses the same state vector and measurements as in the previous one. However, here the estimates of the states are fed back in the DR system to correct the position and the direction of travel [14].
- **Tightly coupled integration:** The state variables are position, speed and angular velocity. The inputs to the Kalman filter are GPS position and in-vehicle sensor data and the DR is, in this case, performed in the Kalman filter. In this approach both systems support each other, in contrast to the loosely coupled methods where the GPS support the DR system. In the tightly coupled approach, an EKF has to be used due to the nonlinearities in the signal model (3.1)-(3.5) [7].

Method:	Error state model	Error state model with feedback	Vehicle state model
Advantages:	A standard Kalman filter can be used, the error variation is relatively low	Errors in the DR stay small	The signal model is valid for large errors
Drawbacks:	The linearisation might get invalid with time (if the errors grow large with time)	Instability and self-oscillations might occur, sensitive to bad measurements, a good signal model is needed	An EKF has to be used

Table 3.1. Advantages and drawbacks with the three loosely coupled integration methods.

In the tightly coupled integration approach, the user has to deal with raw GPS pseudoranges and implement a solution to the GPS positioning problem. This makes the tightly coupled approach a computationally intensive method. In that sense, the loosely coupled approach is more straightforward since the position outputs from the GPS receiver can be used instead of the raw measurements. This makes the loosely coupled approach simpler to implement. However, instead this approach sometimes suffers from problems due to the fact that the GPS errors not fulfil the error assumptions used in Kalman filter theory [4].

In the choice between the three loosely coupled approaches mentioned above, there are some issues that have to be considered. The most important of these issues are listed in Table 3.1, which summarizes the results and observations from [2, 4, 14].

3.5 Map matching

One way to increase the accuracy of a positioning system is to add a map matching algorithm. The main idea of map matching is to compare the travelled trajectory with nearby roads, which are stored in a map data base, and to choose the closest match. In the map data base, shape points of the road are stored. These shape points contain information about the road network, such as position and direction of travel. There are several different approaches to map matching and in this section, semi-deterministic and probabilistic algorithms will be discussed.

3.5.1 Semi-deterministic algorithms

The simplest approach to map matching is to compare the estimated position with positions in a road network and snap it to the closest. This algorithm, called point-to-point map matching, is a semi-deterministic map matching algorithm. Point-to-point map matching is easy to implement but suffers from many drawbacks when used in practice. The main problem can be illustrated by a simple example.

Two roads, A and B , and one estimated position, P , are illustrated in Figure 3.4. The two roads consist of the shape points A^0, A^1, A^2, B^0 and B^1 . It is clear that the position P is closer to road B than to road A . But due to the fact that P is closer to A^1 than it is to either of B^0 or B^1 , the position will be snapped to A^1 . This problem could be solved by introducing more shape points on the road, but this will lead to an increased network and there is always a limit of how many shape points that can be stored.

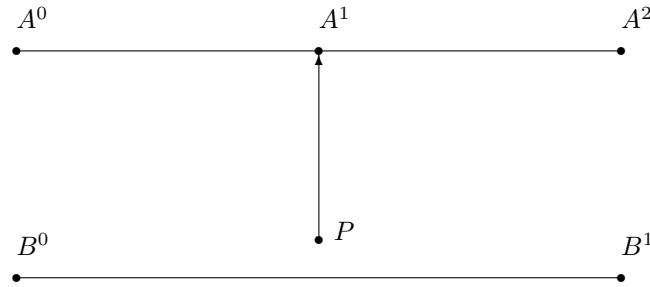


Figure 3.4. The estimated position P is closer to road B , but is incorrectly snapped to road A by the point-to-point map matching algorithm.

Instead of just comparing the estimated position with the shape points, it is more natural to find out which road that it is closest to. If the road is supposed to be piecewise linear between the shape points, it is possible to find out which line segment that has the minimum distance to the estimated position. The point on this line which is closest to the estimated position is chosen as the match. This algorithm, point-to-curve map matching, is a better approach than the point-to-point map matching algorithm, but it also suffers from drawbacks. First, it does not take any historical data into consideration, and this can lead to problems. Consider the following example.

Two roads, A and B , and a sequence of estimated positions, P^0, P^1 and P^2 , are illustrated in Figure 3.5. P^0 and P^1 are snapped to road A , but P^2 can be

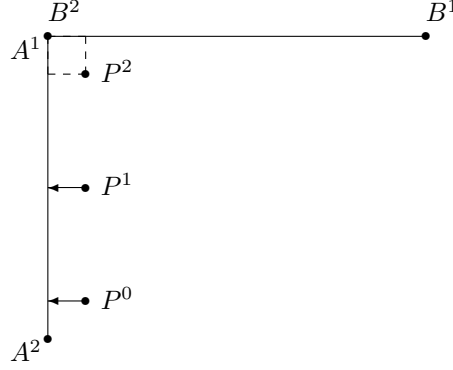


Figure 3.5. The point P^2 could be matched to either road A or road B in a point-to-curve algorithm, but if this algorithm had made use of historical data, P^2 would be snapped to road A .

snapped to either road A or road B , because the distances to the roads are equal. However, if the algorithm had made use of the historical data, the road A would have been chosen as the match.

Another problem with this algorithm is that it can be quite unstable. Suppose that a sequence of estimated positions is close to two different roads. Some of the estimated positions are slightly closer to one of the roads, and some of the positions are slightly closer to the other road. This implies that the matched positions will oscillate between these two roads. This problem is illustrated in Figure 3.6.

A third semi-deterministic approach is the curve-to-curve map matching algorithm. This algorithm considers a sequence of estimated positions and matches this curve to the closest road. There are different ways to define closest; one is to measure the average distance between two curves. This algorithm gives better results than point-to-point map matching and point-to-curve map matching. However, this algorithm also suffers from some drawbacks, for example, when curves of different lengths are compared. More information on semi-deterministic algorithms can be found in [1].

3.5.2 Probabilistic algorithms

An alternative to the semi-deterministic map matching algorithms is probabilistic algorithms. In probabilistic algorithms, some information about the accuracy of the estimated position is needed. If a Kalman filter is used, this is very convenient

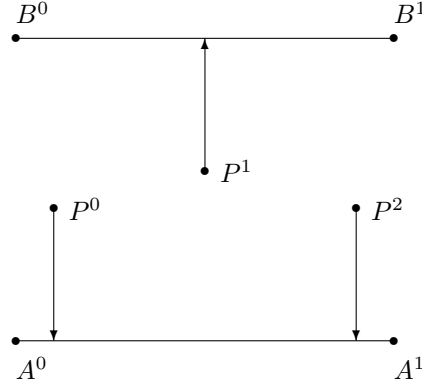


Figure 3.6. When a sequence of estimated positions is close to two roads, the matched position from a point-to-curve algorithm might oscillate between the two roads.

because the covariance of the estimation error is available as a by-product of the filter computations. This covariance information can be used to make a confidence region, which sets the boundary within which the true vehicle position lies with a certain probability. The confidence region is superimposed on the road network and the shape points that fit in this region are selected. The selected shape points are evaluated further in order to determine which of these points that is the most probable location for the vehicle.

There are many aspects that have to be taken into account in this comparison. The shape point that is closest to the estimated position is of course a probable candidate. If the heading is stored in the shape point, this could be compared with the heading of the vehicle. The comparison of the headings is a very important criterion, especially at road intersections. Another aspect is that if the shape point is on the same road as the previous matched position, this shape point is more probable to be the correct position than a shape point on another road. This is because the vehicle is most likely to travel on the same road as it did at the time for the last matching occasion. If there is no shape point in the confidence region of the estimated position, then the estimated position itself is chosen. The fact that it is possible to travel outside the known road network and still get a good estimation of the position is one of the big advantages of the probabilistic algorithm. To learn more about the probabilistic algorithm, see [15].

Chapter 4

State Estimation Theory

In this thesis, DR is integrated with GPS. As mentioned in Section 3.4, one possible integration approach is to use a Kalman filter and in this chapter the Kalman filter theory will be discussed. The presentation of linearised Kalman filters in Section 4.4 and extended Kalman filters (EKF) in Section 4.5 is similar to the one in [12].

4.1 State space description

Many physical systems can be described by a system of first order differential equations or, in the discrete-time case, by difference equations. If these equations can be structured in a certain way, the resulting model is called a state space description and it can be written as

$$x_{k+1} = F_k x_k + G w_k \quad (4.1)$$

$$y_k = H_k x_k + e_k \quad (4.2)$$

where x_k is the state vector and y_k is the output of the system. The process noise w_k and the measurement noise e_k are random processes with the following properties

$$E(w_k) = 0 \quad (4.3)$$

$$E(e_k) = 0 \quad (4.4)$$

$$E(w_k w_k^T) = Q_k \quad (4.5)$$

$$E(e_k e_k^T) = R_k \quad (4.6)$$

$$E(w_k w_{k+i}^T) = 0, \quad i \neq 0 \quad (4.7)$$

$$E(e_k e_{k+i}^T) = 0, \quad i \neq 0 \quad (4.8)$$

$$E(w_j e_k^T) = 0 \quad (4.9)$$

where $E(x)$ is the expectation of x .

4.2 Observers

In most physical systems, it is not possible to measure the state vector. In order to still be able to observe the state variables, the states have to be reconstructed. The reconstruction of the state variables is often done with an observer. A simulation of the system (4.1) can be written as

$$\hat{x}_{k+1} = F_k \hat{x}_k \quad (4.10)$$

and in this way, the state estimate \hat{x}_k is generated. The difference $y_k - H\hat{x}_k$ is a measure of how well the states have been estimated and it is usually referred to as the innovation. If \hat{x}_k is equal to x_k and no measurement noise exists, this difference is zero. If the difference is used as feedback to the simulated system (4.10), the observer

$$\hat{x}_{k+1} = F_k \hat{x}_k + K_k(y_k - H\hat{x}_k) \quad (4.11)$$

is formed, where K_k is a gain matrix. The problem is how to choose K_k . Since the purpose is to get \hat{x}_k close to x_k the estimation error

$$\tilde{x}_k = x_k - \hat{x}_k \quad (4.12)$$

is an interesting variable. This expression combined with (4.1), (4.2) and (4.11) gives

$$\tilde{x}_{k+1} = (F_k - K_k H_k) \tilde{x}_k + G w_k - K_k e_k \quad (4.13)$$

The goal in the observer design process is to find an optimal K_k . A large K_k gives a high adaptation rate in the estimates of the state variables, i.e. the ability to follow rapid changes is good, but it will on the other hand make the estimates more noisy because e_k is multiplied with K_k too. The choice of K_k is therefore always a compromise between these two factors [5].

4.3 Kalman filtering

If the disturbances w_k and e_k are white noises with known intensities, the observer that minimizes the estimation error $\tilde{x}_k = x_k - \hat{x}_k$, in a least mean square error sense, is given by (4.11) where K_k is

$$K_k = P_k H_k^T (H_k P_k H_k^T + R_k)^{-1} \quad (4.14)$$

and where P_k is the positive semi-definite solution to

$$P_k = F_k P_k F_k^T + G_k Q_k G_k^T - F_k K_k (F_k P_k H_k^T)^T \quad (4.15)$$

The matrix P_k is equal to the covariance matrix of \tilde{x}_k and the matrix K_k in (4.14) is known as the Kalman gain. The matrices Q_k and R_k are the intensities of the disturbances w_k and e_k , respectively, but can also be used as design parameters in the design process. An observer where the gain matrix is equal to the Kalman

gain is called a Kalman filter [5].

If the dynamics of the system vary with time, a time-varying Kalman filter is needed. The system matrices are then calculated at every sample, which means that K_k has to be calculated recursively.

4.4 Linearised Kalman filters

If the system dynamics are nonlinear, the system can be described as

$$x_{k+1} = f_k(x_k) + G_k w_k \quad (4.16)$$

$$y_k = h_k(x_k) + e_k \quad (4.17)$$

where f_k and h_k are nonlinear functions. Here, the system has to be linearised. A common approach is to linearise (4.16) and (4.17) around a known nominal trajectory

$$x_{k+1}^{nom} = f_k(x_k^{nom}) \quad (4.18)$$

$$x_0^{nom} = \bar{x}_0 \quad (4.19)$$

This nominal trajectory can be used to express a similar, true trajectory x_k as

$$x_k = x_k^{nom} + \delta x_k \quad (4.20)$$

where x_k^{nom} is the nominal trajectory and δx_k measures the error between the nominal and the true trajectory. If the functions $f_k(x_k)$ and $h_k(x_k)$ are assumed to be smooth functions, they can be approximated with first order Taylor expansions

$$f_k(x_k) \approx f_k(x_k^{nom}) + F_k \delta x_k \quad (4.21)$$

$$h_k(x_k) \approx h_k(x_k^{nom}) + H_k \delta x_k \quad (4.22)$$

where the matrices F_k and H_k are defined by

$$F_k = \left. \frac{\partial f_k(x)}{\partial x} \right|_{x=x_k^{nom}} \quad (4.23)$$

$$H_k = \left. \frac{\partial h_k(x)}{\partial x} \right|_{x=x_k^{nom}} \quad (4.24)$$

The linearised equations about the nominal values can now be written as

$$\delta x_{k+1} = F_k \delta x_k + G_k w_k \quad (4.25)$$

$$y_k - h_k(x_k^{nom}) = H_k \delta x_k + e_k \quad (4.26)$$

The equations (4.25) and (4.26) are linear and hence the standard Kalman filter equations can be used to estimate δx_k . An approximate estimator for δx_k , with

initial estimate $\delta\hat{x}_{k|k-1} = \delta\hat{x}_0 = 0$ and $P_{k|k-1} = P_0$, can be recursively computed as follows

$$\delta\hat{x}_{k+1|k} = F_k \delta\hat{x}_{k|k} \quad (4.27)$$

$$\delta\hat{x}_{k|k} = \delta\hat{x}_{k|k-1} + K_k (y_k - h_k(x_k^{nom}) - H_k \delta\hat{x}_{k|k-1}) \quad (4.28)$$

$$K_k = P_{k|k-1} H_k^T (H_k P_{k|k-1} H_k^T + R_k)^{-1} \quad (4.29)$$

$$P_{k|k} = (I - K_k H_k) P_{k|k-1} \quad (4.30)$$

$$P_{k+1|k} = F_k P_{k|k} F_k^T + G_k Q_k G_k^T \quad (4.31)$$

If x_k^{nom} is added to the estimate $\delta\hat{x}_k$, an estimate of x_k has been found

$$\hat{x}_k = x_k^{nom} + \delta\hat{x}_k \quad (4.32)$$

The problem with the linearised Kalman filter is that the error between the nominal and the true trajectory tends to increase with time. As this error grows, the significance of the higher order terms in the Taylor series expansion grows. If the error increases too much, the approximations in (4.21)–(4.22) are not good enough [6].

4.5 Extended Kalman filters

One way to get around the problem with the error growth with time in the previous section is to linearize around the estimated trajectory instead of around a nominal trajectory. This idea was first suggested by E.F. Schmidt and the resulting filter is thus called the “Kalman-Schmidt” filter or, alternatively, the extended Kalman filter (EKF) [6]. The EKF can lead to smaller errors between the estimated trajectory, which f_k and g_k are linearised around, and the true trajectory. This is due to the fact that the EKF only uses linear approximation over the state estimation errors in contrast to the linearised approach, which uses linear approximation both over the state estimation errors and the error between the nominal trajectory and the estimated trajectory. In the EKF, the approximations have the following appearance

$$f_k(x_k) \approx f_k(\hat{x}_{k|k}) + F_k(x_k - \hat{x}_{k|k}) \quad (4.33)$$

$$h_k(x_k) \approx h_k(\hat{x}_{k|k-1}) + H_k(x_k - \hat{x}_{k|k-1}) \quad (4.34)$$

$$F_k = \left. \frac{\partial f_k(x)}{\partial x} \right|_{x=\hat{x}_{k|k}} \quad (4.35)$$

$$H_k = \left. \frac{\partial h_k(x)}{\partial x} \right|_{x=\hat{x}_{k|k-1}} \quad (4.36)$$

Using (4.33)–(4.36), (4.16) and (4.17) can be approximated as

$$x_{k+1} = F_k x_k + (f_k(\hat{x}_{k|k}) - F_k \hat{x}_{k|k}) + G_k w_k \quad (4.37)$$

$$y_k = (h_k(\hat{x}_{k|k-1}) - H_k \hat{x}_{k|k-1}) + H_k x_k + e_k \quad (4.38)$$

This is a linear state-space model for x_k and therefore the standard Kalman filter equations can be used for this system. An approximate estimator for x_k , with initial state $\hat{x}_{k|k-1} = \hat{x}_0$ and $P_{k|k-1} = P_0$, can be recursively computed as follows

$$\hat{x}_{k+1|k} = f_k(\hat{x}_{k|k}) \quad (4.39)$$

$$\hat{x}_{k|k} = \hat{x}_{k|k-1} + K_k(y_k - h_k(\hat{x}_{k|k-1})) \quad (4.40)$$

$$K_k = P_{k|k-1} H_k^T (H_k P_{k|k-1} H_k^T + R_k)^{-1} \quad (4.41)$$

$$P_{k|k} = (I - K_k H_k) P_{k|k-1} \quad (4.42)$$

$$P_{k+1|k} = F_k P_{k|k} F_k^T + G_k Q_k G_k^T \quad (4.43)$$

For the linearised Kalman filter, if a nominal trajectory is known before the system is used, a great advantage for real-time implementation can be made by precomputing the measurement matrices, system matrices and Kalman gain matrices. However, this precomputing is only possible for the linearised Kalman filter. It is not possible for the EKF because the measurement matrices, system matrices and Kalman gain matrices all depend on the real-time state estimates [6].

Neither the linearised Kalman filter nor the EKF is optimal in the same sense as the standard Kalman filter is optimal for a linear system.

Chapter 5

Measurements and Data Acquisition

In order to perform DR, the speed, yaw rate and pitch rate are needed. As mentioned in Section 3.2 these signals can be derived from a speedometer and a gyroscope. To integrate the output from the DR system with a GPS, the position from a GPS receiver is needed. In this chapter the data acquisition, some characteristics of the in-vehicle sensors and limitations due to data errors are described.

5.1 Data acquisition

In this project, two different routes have been used for data acquisition. The first route is 25 km long and is located on the countryside outside Gothenburg. The second route is located in a suburban area in Gothenburg and is 6 km long and contains a 2060 m long tunnel.

The test vehicle that has been used to collect data from these routes is a Volvo S80, equipped with a gyroscope, a speedometer and a GPS receiver. The gyroscope is a low cost automotive gyroscope and was mounted on a portable platform installed in the boot of the test vehicle. The speedometer signal has been taken from the Controller Area Network (CAN) bus, which is an electronic network used for information communication between different components and systems in the vehicle. The GPS receiver that has been used is a Garmin GPSMAP 76S receiver and the GPS antenna has been placed in the centre of the top of the vehicle. All signals have been sampled with a frequency of 50 Hz, but the GPS signal was only updated with about 0.5 Hz. The data were collected and stored with an industrial PC and Volvo ERS Logger, which is an internal data collection program, installed on a laptop.

5.2 GPS measurements

During the test drives, position, heading, speed and dilution of precision (DOP) have been sampled from the GPS receiver. This device expresses the position in WGS-84-coordinates, the speed in m/s and the heading in radians. The GPS positions have an accuracy, 95% of the times, of 15 m in the north-east plane and 30 m in the height component [10]. The GPS resolution is about 1.8 m in north-south direction and 0.9 m in east-west direction (the limiting factor in the resolution is the interface between the GPS receiver and the PC). An undesirable GPS feature, from a positioning system designer's point of view, is that data are delivered at a different frequency from time to time. As can be seen in Figure 5.1, the time between two subsequent position updates can differ as much as 0.7 s. Unfortunately, the

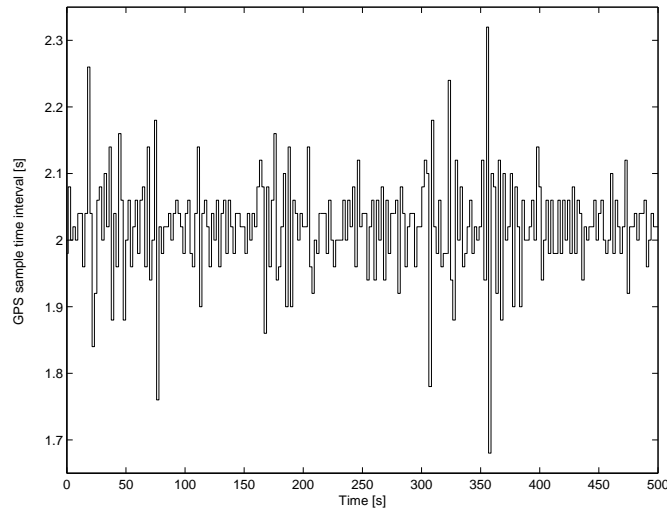


Figure 5.1. The GPS update time intervals during the first 500 s of route 1.

GPS receiver does not give any information about the update frequency. An even worse property is that the position delivered at time k might derive from any time instant between $k - 1$ to k (where k is the update time for the latest GPS position).

Another undesirable feature with Garmin GPSMAP 76 S is that when GPS signal masking occurs, the receiver continues to deliver an estimated position, which is just an extrapolation of the latest GPS positions. The receiver does not provide the user with information about whether the GPS position is an estimated position or not. Once the GPS receiver starts to extrapolate the positions, it will present constant speed, DOP and heading values.

5.3 In-vehicle sensor measurements

The speed that is used to perform the DR, is the speed provided by the vehicle's speedometer, which express the speed in m/s. A description of the functionality of a speedometer is given in Section 3.2.2. The speedometer signal has a resolution of $2.7 \cdot 10^{-3}$ m/s and is updated with a frequency of approximately 70 Hz. The gyroscope, used for yaw rate and pitch rate measurements can measure angular velocities around two axes and is designed to be used for stability programs. The gyroscope has a resolution of $3.15 \cdot 10^{-3}$ rad/s and is updated with a frequency higher than 50 Hz. The gyroscope offset has a magnitude between 10^{-2} and 10^{-3} rad/s.

5.4 Limitations due to data errors

The single most limiting factor, with respect to overall system performance, is the fact that the time which the GPS position derives from is not known exactly. The use of an inaccurate time stamp for the GPS position will lead to the use of an inaccurate position. The worst case scenario is that the GPS position is considered to be a real-time measurement when it actually derives from the time when the last GPS position was delivered (or vice versa). Since the GPS update frequency is approximately 0.5 Hz, this would lead to an uncertainty in the position with about two times the value of the current speed. If the innovation in the Kalman filter is based on an incorrectly measured position, this will of course affect the system performance.

Another limitation is that during GPS signal masking, the receiver continues to deliver a predicted position without giving any explicit information about this change in the signal quality. However, using the fact that some GPS signals, like the speed, are constant as soon as the GPS receiver predicts the position, the GPS information can be ignored when this happens. The problem is that it takes two samples in the filter to detect the constant signals. This means that two incorrect positions will be used and this is of course going to affect the estimation of the gyroscope offsets and thus also the overall performances during GPS signal masking.

5.5 DR and GPS trajectories

The DR trajectory that can be constructed from the raw measurements, without using any technique for compensation for the gyroscope offset, will drift away from the true position. The gyroscope offset in the yaw rate measurements will lead to a drift in the north-east plane. The drift in the DR system can be studied by comparing the DR trajectory with the GPS trajectory. As can be seen in Figure 5.2, the drift when DR is performed with raw measurements is considerable for the gyroscope used in this thesis.

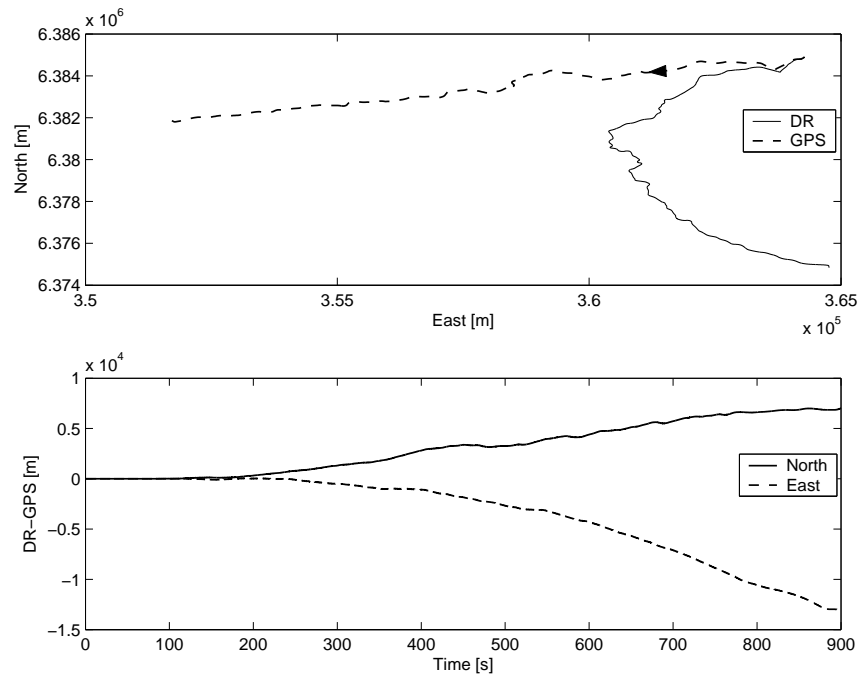


Figure 5.2. The GPS trajectory compared to the DR trajectory (top), when DR is performed with raw measurements from the first 900 s of route 1 and the difference between the GPS and the DR trajectories (bottom). The arrow indicates the direction of travel.

Chapter 6

Positioning System with Complete Vehicle State Model

In order to determine an absolute position, with high frequency and under GPS signal masking, DR and GPS can be integrated. The integration can, for example, be done with a Kalman filter. There are, as mentioned in Section 3.4, different Kalman filter integration approaches and in this chapter, the complete vehicle state model approach and the evaluation of it is presented.

6.1 Complete vehicle state model

The integration approach with a complete vehicle state model, which is discussed in Section 3.4, is the approach chosen in this thesis for integration of DR and GPS. The state equations for this approach are obtained by using the equations describing the movement of the vehicle, see Section 3.1, to which the sensor error models are added. In the next three sections, the sensor error models used in this thesis are described.

6.1.1 Gyroscope error model

Several gyroscope errors were mentioned in Section 3.2.1. However, not all of these errors are relevant for the gyroscope used in this thesis. The errors used for modelling the gyroscope errors are nonlinearity, measurement noise, misalignment, quantization and offset. All these errors, except gyroscope offset, are simply modelled as white Gaussian noise. The offset is varying slowly and is thus modelled as a random walk process. Random walks are cumulative sums of white noise. The

equations for the gyroscope offset can be written as

$$\Delta_{\dot{\psi}}(k+1) = \Delta_{\dot{\psi}}(k) + w_{\dot{\psi}} \quad (6.1)$$

$$\Delta_{\dot{\theta}}(k+1) = \Delta_{\dot{\theta}}(k) + w_{\dot{\theta}} \quad (6.2)$$

where $\Delta_{\dot{\psi}}$ is the yaw rate offset and $\Delta_{\dot{\theta}}$ is the pitch rate offset. The signals $w_{\dot{\psi}}$ and $w_{\dot{\theta}}$ are white Gaussian noises.

The specification of the gyroscope gives the following approximate intensities of the errors in the gyroscope

$$nonlinearity = 1 \cdot 10^{-5}$$

$$measurement\ noise = 1 \cdot 10^{-4}$$

$$misalignment = 1 \cdot 10^{-6}$$

$$quantization = 1 \cdot 10^{-5}$$

The intensities of $w_{\dot{\psi}}$ and $w_{\dot{\theta}}$ are initially set to $1 \cdot 10^{-4}$.

6.1.2 Speedometer error model

The uncertainty in radii of the vehicle's wheels, measurement noise and quantization effects give rise to speedometer errors. The uncertainty in radii gives rise to a speed scale error (S), which is modelled as a random walk process

$$S(k+1) = S(k) + w_S \quad (6.3)$$

where w_S is white Gaussian noise.

The other speedometer errors are modelled as white Gaussian noise. The speedometer error intensities were approximated with the following values

$$measurement\ noise = 1 \cdot 10^{-3}$$

$$quantization = 1 \cdot 10^{-5}$$

The intensity of w_S is given the value $1 \cdot 10^{-4}$.

6.1.3 GPS error model

The accuracy of the GPS position is affected by errors as range errors and geometric errors, as mentioned in Section 3.3. These errors can, for example, be modelled, as the errors in the DR with an error state description or measurement noise. The GPS errors are here modelled as measurement noise and the intensities of the GPS errors will thus contribute to the R matrix in the Kalman filter equations. The uncertainties in the GPS measurements are given in Section 5.2 and are 15 m in the north and east plane and 30 m in the height component. The uncertainty in the GPS measurements increase with increasing DOP value and the DOP value is therefore included in the R matrix.

6.1.4 Complete vehicle state equations

The equations describing the movement of the vehicle and the sensor error models give the following state equations

$$N(k+1) = N(k) + v(k)T\cos(\Theta(k))\cos(\Psi(k)) + w_1 \quad (6.4)$$

$$E(k+1) = E(k) + v(k)T\cos(\Theta(k))\sin(\Psi(k)) + w_2 \quad (6.5)$$

$$Z(k+1) = Z(k) + v(k)T\sin(\Theta(k)) + w_3 \quad (6.6)$$

$$\Psi(k+1) = \Psi(k) + T\dot{\Psi}(k) + w_4 \quad (6.7)$$

$$\Theta(k+1) = \Theta(k) + T\dot{\Theta}(k) + w_5 \quad (6.8)$$

$$\dot{\Psi}(k+1) = \dot{\Psi}(k) + w_6 \quad (6.9)$$

$$\dot{\Theta}(k+1) = \dot{\Theta}(k) + w_7 \quad (6.10)$$

$$\Delta_{\dot{\Psi}}(k+1) = \Delta_{\dot{\Psi}}(k) + w_8 \quad (6.11)$$

$$\Delta_{\dot{\Theta}}(k+1) = \Delta_{\dot{\Theta}}(k) + w_9 \quad (6.12)$$

$$v(k+1) = v(k) + w_{10} \quad (6.13)$$

$$S(k+1) = S(k) + w_{11} \quad (6.14)$$

The definitions of N , E , Z , Ψ , Θ , $\dot{\Psi}$, $\dot{\Theta}$ and v can be found in Section 3.1.

This signal model is nonlinear and cannot be used directly in a Kalman filter. In order to be able to use a nonlinear signal model, a linearised Kalman filter or an EKF has to be used. If the linearised Kalman filter approach is used, the problem with the divergence of the nominal trajectory from the true trajectory mentioned in Section 4.4 will occur and therefore an EKF has been used.

6.2 Implementation of the complete vehicle state model

A positioning system with a complete vehicle state model has been implemented in Simulink. The DR is performed according to the description in Section 3.1. The EKF in the positioning system is based on the signal model stated in the previous section, which gives the following state vector

$$x = (N \ E \ Z \ \Psi \ \Theta \ \dot{\Psi} \ \dot{\Theta} \ \Delta_{\dot{\Psi}} \ \Delta_{\dot{\Theta}} \ v \ S)^T$$

An overview of the system is presented in Figure 6.1. The DR in the positioning system is performed with the frequency at which the speed and yaw rate measurements are sampled with. This frequency has to be set by the system user before the system is started and is in this thesis set to 50 Hz. To perform DR, an initial position and attitude have to be given. The DR position and yaw angle are

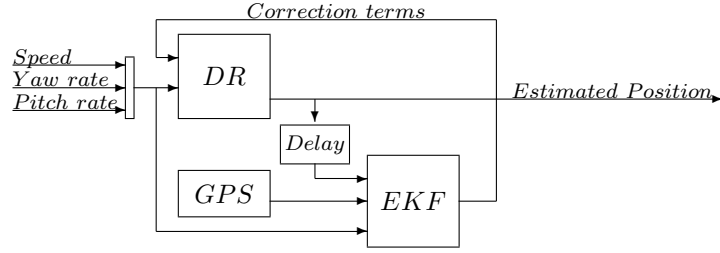


Figure 6.1. A schematic overview of the positioning system with a complete vehicle state model. The correction terms are the estimated position, attitude, offsets and speed scale factor.

initialised with the first GPS position and heading, respectively. The pitch angle is initialised as zero. In order to be able to compare the GPS position with the calculated position from the DR, the GPS position is transformed from WGS-84 to UTM coordinates with the expressions in Appendix B.1. In the EKF, the GPS position, GPS heading, yaw rate, pitch rate and the speed are used as measurements and the nonlinear measurement equations are formed as

$$GPS_N(k) = N(k) + e_1 \quad (6.15)$$

$$GPS_E(k) = E(k) + e_2 \quad (6.16)$$

$$GPS_Z(k) = Z(k) + e_3 \quad (6.17)$$

$$\dot{\Psi}_{measured}(k) = \dot{\Psi}(k) + \Delta_{\dot{\Psi}} + e_4 \quad (6.18)$$

$$\dot{\Theta}_{measured}(k) = \dot{\Theta}(k) + \Delta_{\dot{\Theta}} + e_5 \quad (6.19)$$

$$GPS_{heading}(k) = \Theta(k) + e_6 \quad (6.20)$$

$$v_{measured}(k) = v(k)S(k) + e_7 \quad (6.21)$$

where $\dot{\Psi}_{measured}$ and $\dot{\Theta}_{measured}$ are the mean values of the measured angular velocities under the time interval between two GPS measurements. $GPS_{heading}$ is the heading provided by the GPS receiver and $v_{measured}$ is the average speed from the speedometer under the same time interval as above. The reason for introducing mean values as proposed is to get measurements that better describe the movement of the vehicle since the last GPS measurement.

The functions and matrices f , h , F , H , G , Q and R are needed in the EKF equations and are defined as in Section 4.5. The F , H and G matrices can be found in Appendix A.1. The function $f(x)$ is the right hand side of (6.4)–(6.14) without the w :s and is needed for the time update, described by 4.39. In order to use the latest measurements of yaw rate, pitch rate and speed, the position and attitude calculated in the DR are used in the EKF for the time update of the position and the attitude. The function $h(x)$ is the right hand side of (6.15)–(6.21) without the e :s. The Q and R matrices in the EKF equations describe how the process and

measurement noise affect the state and observation variables, respectively. These matrices can be, and are in this thesis, used as design parameters. However, to get a starting point in the design process, the position (i, i) in the Q matrix is given the value of the intensity of the white noise w_i , which is approximated with the uncertainty in Equation i of (6.4)–(6.14). The R matrix is formed in a similar way as the Q matrix. To get the starting values for the R matrix the uncertainties in (6.15)–(6.21) are used as the diagonal elements in the R matrix.

The filter estimates are used to correct the position, yaw and pitch angles in the DR and to correct measurements of yaw rate, pitch rate and speed used there. These estimates are, however, not given in real-time, but with the unknown time delay of the GPS position measurement (t_{gps}), mentioned in Section 5.2. The fact that the GPS position at time k is a delayed measurement, i.e. it derives from the time $k - t_{gps}$, is the reason why the estimates are not a real-time estimates. In order to make the EKF equations consistent, all others measurements must be from the time $k - t_{gps}$. When the estimates are used to correct the DR, consideration has to be taken to t_{gps} . The position, the yaw angle and the pitch angle estimates at time k have to be used to correct DR values from time $k - t_{gps}$. The term used to correct the DR position at time k is created by taking the difference between the DR position at time $k - t_{gps}$ and the estimated position at time k . This correction term is then added to the DR position at time k . The equations describing this are

$$\begin{aligned} DR_N(k) &= DR_N(k) + (DR_N(k - t_{gps}) - N(k)) \\ DR_E(k) &= DR_E(k) + (DR_E(k - t_{gps}) - E(k)) \\ DR_Z(k) &= DR_Z(k) + (DR_Z(k - t_{gps}) - Z(k)) \end{aligned}$$

where DR_N , DR_E and DR_Z are the north, east and height position coordinates in the DR. To avoid abrupt movements in the position, the whole correction is not made in one sample, but instead ramped up during one second.

The estimates of the yaw angles are used to correct the calculated yaw angles in the DR. This is done by setting the yaw angle in the DR, at time k , to the sum of the yaw angle estimate and change in yaw angle from time $k - t_{gps}$ to k . The pitch angle estimates are used similarly in the DR. The angle corrections are described by

$$\begin{aligned} DR_\Psi(k) &= \Psi(k) + (DR_\Psi(k) - DR_\Psi(k - t_{gps})) \\ DR_\Theta(k) &= \Theta(k) + (DR_\Theta(k) - DR_\Theta(k - t_{gps})) \end{aligned}$$

where DR_Ψ and DR_Θ are the yaw angle and pitch angle calculated in the DR, respectively.

The estimated offsets of yaw rate, pitch rate and speed scale factor can approximately be considered as real-time estimates, due to the fact that the offsets and speed scale factor are considered to be varying slowly. These estimates are used to

correct the measured yaw rate, pitch rate and speed, respectively. This is described with the following expressions

$$\begin{aligned}\dot{\Psi}_{corrected}(k) &= \dot{\Psi}_{measured}(k) - \Delta_{\dot{\Psi}}(k) \\ \dot{\Theta}_{corrected}(k) &= \dot{\Theta}_{measured}(k) - \Delta_{\dot{\Theta}}(k) \\ v_{corrected}(k) &= v_{measured}(k)/S(k)\end{aligned}$$

Here, $\dot{\Psi}_{corrected}$ and $\dot{\Theta}_{corrected}$ are the corrected measurements of the yaw and pitch rate while $v_{corrected}$ is the corrected measurement of the speed. These are the signals used to perform the DR.

The estimates of yaw rate, pitch rate and speed are only used internally in the Kalman filter. The delay t_{gps} is unknown and varies from one sample to another. However, in this thesis, the value of t_{gps} has been set to a constant value in the model.

To initialize the filter, the P matrix and the state variables have to be given initial values as

$$P(0| - 1) = P_0 \quad (6.22)$$

$$\hat{x}(0| - 1) = x_0 \quad (6.23)$$

where \hat{x} is the estimated state vector.

The N , E and Z states are initialised with the first DR position available (the DR is started before the filter and initialised, as mentioned above, with the first GPS position). The Ψ and Θ states are initialised with the first yaw angle and pitch angle from the DR. The remaining states are initialised as zero. Since P_0 is affecting the transient behavior of the filter, it will be considered as a design parameter.

The Kalman filter is disabled when the speed is zero and when GPS signal masking occurs. As mentioned in Section 5.2, GPS signal masking can be detected by using the fact that the GPS speed, GPS heading and DOP are all constant values during signal masking. During GPS signal masking, DR is performed with measured signals that are corrected with the latest estimates. After a period of GPS signal masking, the filter is restarted with position, yaw angle and pitch angle from the DR block and the yaw rate, pitch rate, offsets, speed and speed scale factor from the last state estimate made by the filter before the GPS signal masking occurred. Here, the latest measurements of the speed, yaw rate and pitch rate could be used to restart the filter with, but this has not been done in this thesis. After a GPS signal masking, the P matrix is set to P_0 because the estimate errors are now larger than at the time for the last estimate before GPS signal masking.

The parameters T and t_{gps} have to be defined by the positioning system user before

starting the system. The output from the positioning system can be presented in both WGS-84 coordinates and UTM coordinates.

6.3 Real-time implementation of the complete vehicle state model

A real-time implementation of the positioning system has been done by compiling the Simulink model to C-code. This has been done using Real-Time Workshop, which is a Matlab based compiler. The target for the compiling process is a operating system called xPC and therefore the C-code has to be compiled to xPC-specific machine code. The time needed for processing the model, turned out to be less than 0.02 s, i.e. the positioning system can be processed with 50 Hz. The real-time implementation has been provided with GPS position, GPS heading, speed, yaw rate and pitch rate at a frequency of 50 Hz.

6.4 Limitations of positioning system with vehicle state model

When starting the positioning system, the GPS position, speed, yaw rate and pitch rate have to be available to the system. If these signals are unavailable at the starting time, the positioning system will present an invalid position and the system has to be restarted. If the speed is nonzero when the positioning system is started, the errors during the transient time will be larger than if the system is started when the vehicle is standing still. Another limitation is that the positioning system cannot automatically handle changes of UTM zones. The user has to set which zone is used and when shifting UTM zones the system has to be restarted.

6.5 Evaluation of positioning system with vehicle state model

The previously described positioning system has been tested and evaluated with the test routes described in Section 5.1. During the evaluation, the Q , R and P_0 matrices have been adjusted to make the Kalman filter perform well. The Q , R and P_0 matrices that have been used in this evaluation can be found in Appendix A.2. However, in order to find the optimal values of Q , R and P_0 , more design work has to be done. In this thesis, the evaluation has been done without comparing the estimated position with a true absolute position. Instead, the GPS position has when available, been used as a good approximation of the true position. The DR is initialised with the first GPS position and all corrections done to the DR positions are depending on the GPS position. Hence, the performance of the system with respect to the absolute position accuracy will only depend on the GPS accuracy. The GPS accuracy cannot be affected in this thesis and the positioning output is

therefore never compared with a true absolute position.

The evaluation of the estimates has been done with respect to a number of system characteristics. These characteristics are the ability to follow the GPS signal, the ability to estimate the gyroscope offset, yaw rate, pitch rate and attitude and the ability to handle GPS signal masking. The value of t_{gps} that gives the best system performance has turned out to be 0.5 s, i.e. the GPS position is assumed to be delayed 0.5 s.

6.5.1 Absolute position

The evaluation of the positioning system shows that the system is able to give a satisfactory position solution in the north-east plane. The estimated north and east components are within 10 m from the GPS position after 400s using data from route 1 as input to the system, see Figure 6.2. During the first 400 seconds, the

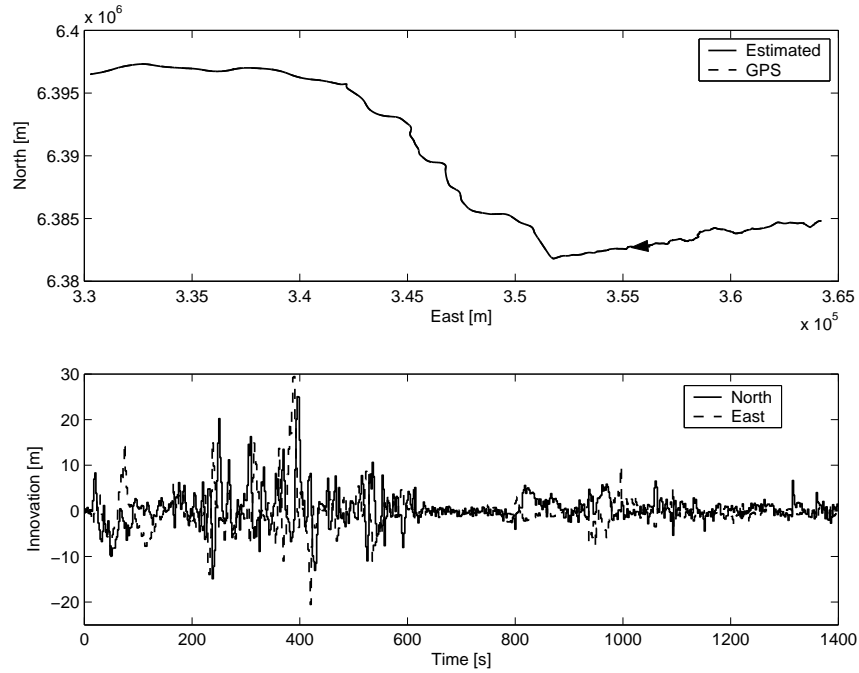


Figure 6.2. The estimated trajectory and the GPS trajectory (top) and the innovation, i.e. the difference between estimated position and GPS position (bottom), from test route 1. The arrow indicates the driving direction.

estimated position diverges up to 30 m from the GPS position. This is due to the

fact that the transient time of the Kalman filter for this route is about 400 s. As can be seen in Figure 6.3, the positioning system delivers a smoother trajectory than the GPS receiver. This is of course because the estimated position is delivered at a higher frequency. In particular, the system gives better estimates at low yaw

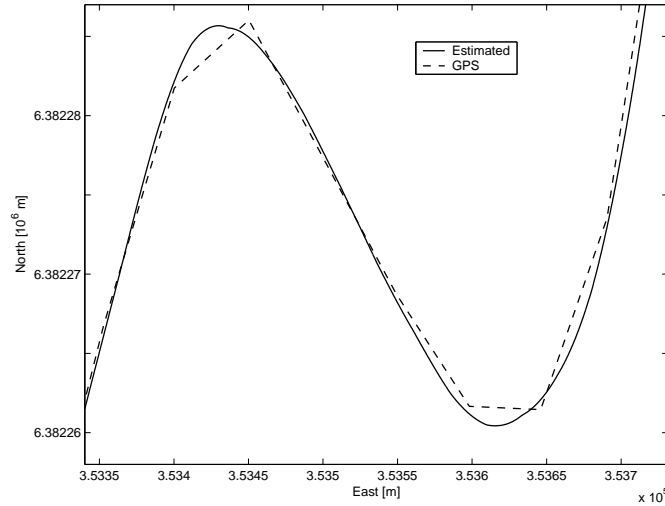


Figure 6.3. Comparison between the estimated trajectory and the GPS trajectory in a curve on route 1.

rates. This can be seen in Figure 6.2 where the errors decrease in magnitude after about 600 s and at this time the yaw rate is considerably lower than the yaw rate between 0 to 600 s, see Figure 6.4.

The positioning system with a complete vehicle state model gives an estimated height component that differs up to 10 m from the GPS height and the system is not able to catch the form of the height component of the driven trajectory. That is, the positioning system cannot deliver an as smooth trajectory for the height component as it can for the north and east components, see Figure 6.5. The reason for this is that the estimated pitch angle is not a satisfactory estimation and this is further discussed in Section 6.5.4. The magnitude of the innovation for the height component is the same as the innovation for the north and the east components, which can be seen in Figure 6.6. This is not a satisfactory result, since the distance travelled between two GPS updates is much shorter for the height component than it is for the north and the east components.

6.5.2 Yaw rate and pitch rate estimation

The positioning system seems to be able to give accurate estimates of the yaw rate. This can be seen in Figure 6.7. The evaluation of the ability of the positioning

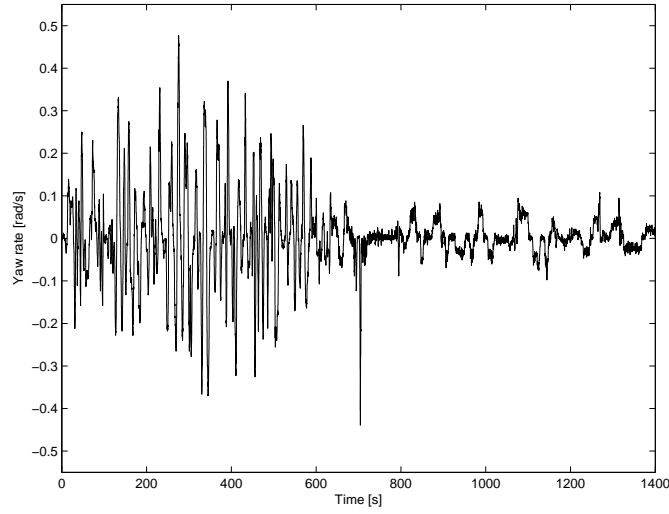


Figure 6.4. Measured yaw rate from route 1.

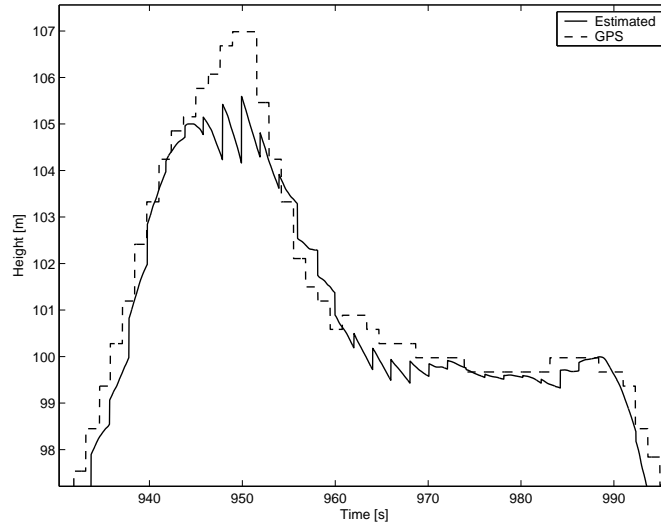


Figure 6.5. The estimated height and the GPS height for a part of route 1.

system to estimate the yaw rate has been done by comparing the estimated and the measured yaw rate. The measured yaw rate, except for an additional offset, is considered to be a good approximation of the true yaw rate. If the estimated yaw rate follows the measured yaw rate with the distinction of no offset being present, the estimated yaw rate is considered as an accurate estimate. The estimated yaw rate has this behavior, as can be seen in Figure 6.7 and is therefore

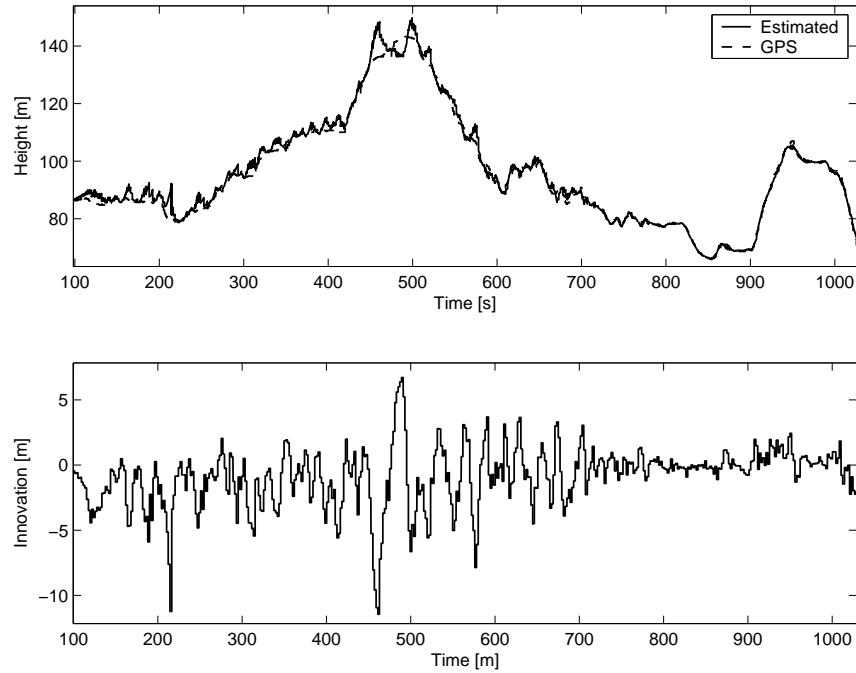


Figure 6.6. The estimated height and the GPS height (top) and the innovation for the height component (bottom) for a part of route 1.

considered to be a satisfactory estimate of the true yaw rate.

The estimated pitch rate differs a lot from the measured pitch rate, which can be seen in Figure 6.8. Even though the measured pitch rate is compensated with an accurate offset, the measured pitch rate cannot be considered to be a good approximation of the true pitch rate. This is, among other things, due to a large process noise in the pitch rate. This process noise derives from an angular velocity which arises from compression of the vehicle's suspensions. This happens, for example, during acceleration and retardation. Therefore, in order to determine whether the estimate is accurate or not, more evaluation work has to be done.

6.5.3 Gyroscope offset estimation

After the filter transient time (about 400 s), the filter gives satisfying estimates of the yaw rate offset and the pitch rate offset. To evaluate if the offsets estimates are satisfying, a qualitative analysis is done. The offset estimate is said to be satisfactory if the estimated offset is slowly varying and stabilized on a value between 10^{-3} and 10^{-2} , which is as mentioned in Section 5.3 the magnitude of the offset. This is, as can be seen in Figure 6.9, the behavior of the estimated yaw rate offset

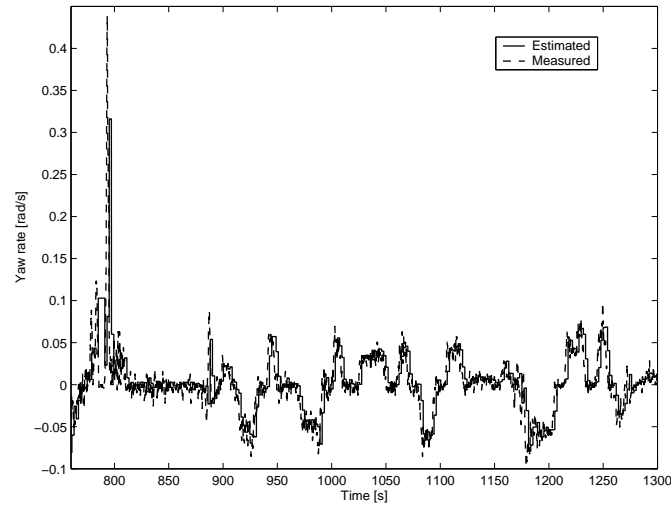


Figure 6.7. Estimated and measured yaw rate for a part of route 1.

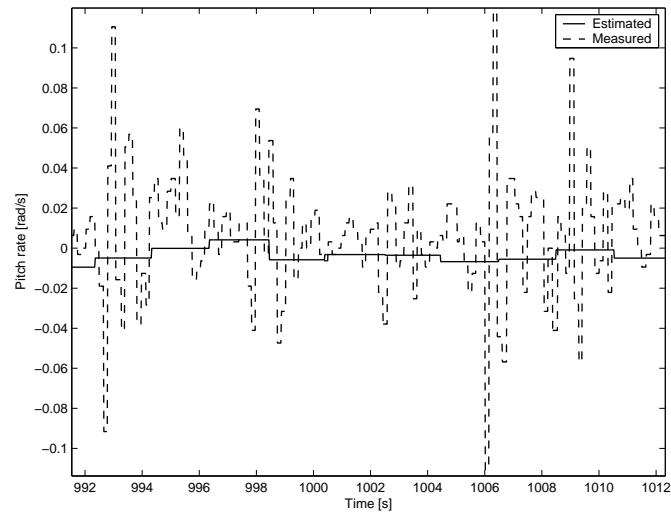


Figure 6.8. Estimated and measured pitch rate for a part of route 1.

and it is therefore said to be satisfactory. In Figure 6.10, a typical sequence of pitch rate offset estimates is illustrated. The estimates of the pitch rate offset are stabilised on a value around $8 \cdot 10^{-3}$, which probably is a good estimate of the real pitch rate gyroscope offset.

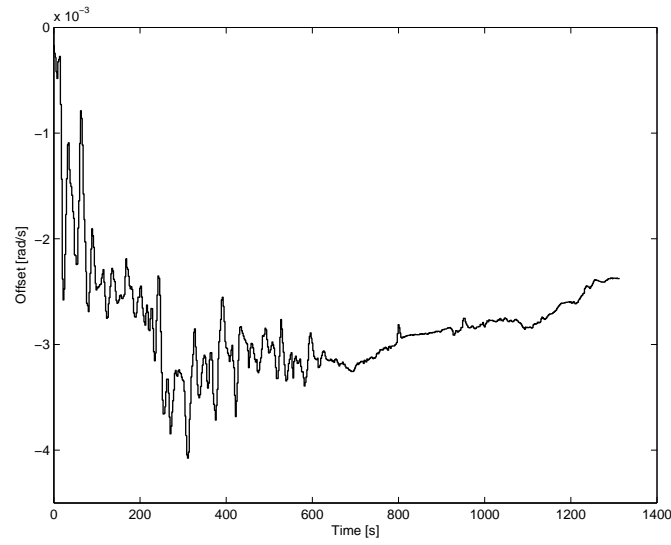


Figure 6.9. Estimated yaw rate offset for route 1.

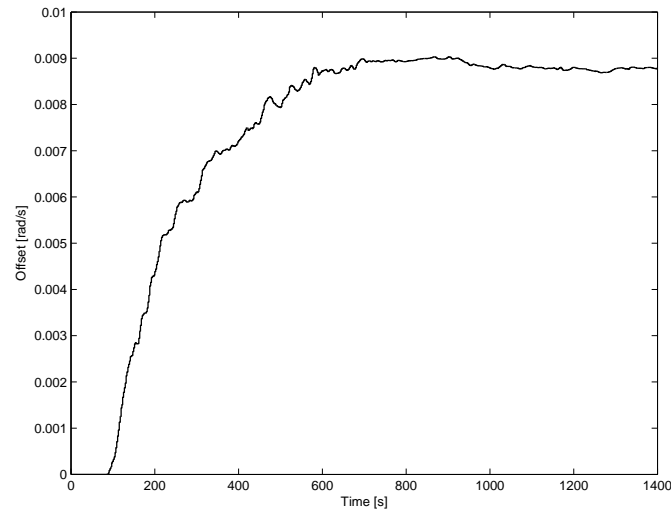


Figure 6.10. Estimated pitch rate offset for route 1.

6.5.4 Attitude estimation

The positioning system seems to be able to estimate the yaw angle accurately. This can be seen in Figure 6.11, where the yaw angle estimates are compared with the GPS heading. This comparison is done in order to get a primary evaluation of the quality of the yaw angle estimate. The drawbacks with the GPS heading signal

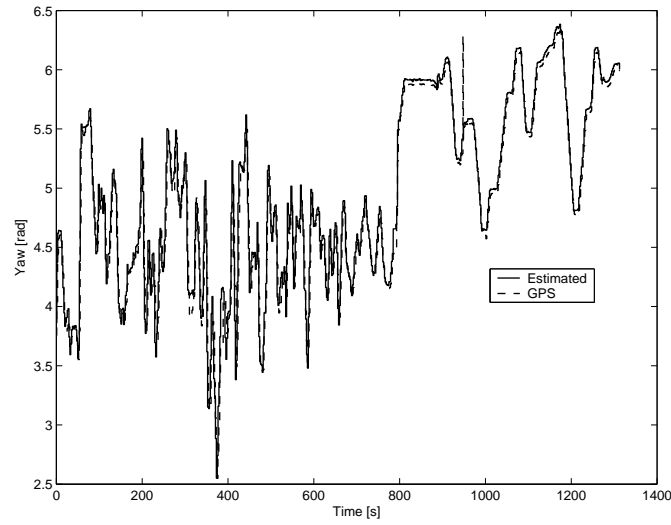


Figure 6.11. Estimated yaw angle and GPS heading for route 1.

is its low resolution, low update frequency and the fact that it is not provided in real-time. Despite this, the GPS heading is a good reference value for the estimated yaw angle. By studying the estimated position, it seems like the yaw angle estimate is satisfactory. The estimated yaw angle is used in the DR, and if this estimate is inaccurate, this will have a negative effect on the accuracy of the estimated position.

The GPS does not deliver a pitch angle and therefore there is no reference signal present that can be compared with the estimated pitch angle. When the estimated pitch angle is used in the DR, this sometimes leads to large differences between the GPS trajectory and the DR trajectory, as can be seen in Figure 6.5. This means that the estimated pitch angle probably is inaccurate.

6.5.5 GPS signal masking

The evaluation of the positioning system indicates that the system can handle GPS signal masking well for a period of time. This ability has been evaluated by using data from route 2, which contains a 2060 m long tunnel. Hence, the measurements from this route contain a 127 s long sequence, starting at 498 s and ending at 625 s, where GPS signal masking occurs. The ability to handle GPS signal masking is evaluated by comparing the estimated position with the GPS position on the other side of the tunnel. As can be seen in Figure 6.12, the estimated position after the tunnel differs about 25 m in both north and east coordinates from the GPS position. The trajectory the GPS receiver estimates when GPS signal masking occurs can be seen at the beginning of the tunnel in Figure 6.12. After a time of signal masking the GPS receiver presents the position as zero. The first GPS measurement after

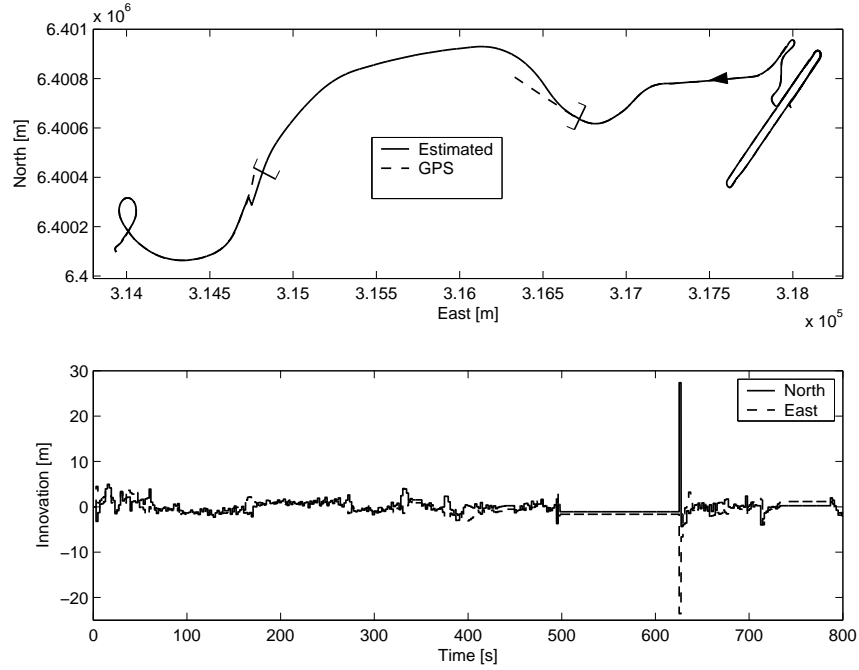


Figure 6.12. The estimated trajectory and the GPS trajectory (top) and the innovations (bottom) from route 2. The brackets indicate the beginning and the end of the tunnel and the arrow indicate the direction of travel.

the GPS signal masking can also be seen in Figure 6.12 just after the end of the tunnel. During the GPS signal masking the extended Kalman filter is disabled and the innovation will therefore remain constant. This means that during GPS signal masking the innovation gives no information about the system performance.

As an indication of the need of the Kalman filter in the case of GPS signal masking, the DR trajectory through the tunnel computed without any offset compensations can be compared with the offset compensated DR trajectory, i.e. the estimated trajectory. Without the use of a Kalman filter (and an offset compensated yaw rate signal) the position error at the end of the tunnel is 400 m wrong in the north coordinate and 300 m in the east coordinate. This can be compared to a 25 m error in both directions when a Kalman filter is used. The different trajectories can be seen in Figure 6.13. As discussed in Section 6.5.4, the system does not estimate the pitch angle satisfactory. This gives that the error in the estimated height component will grow large with time during GPS signal masking.

Other circumstances than the conditions present during route 2 will of course give different performance during GPS signal masking, either better or worse. In Fig-

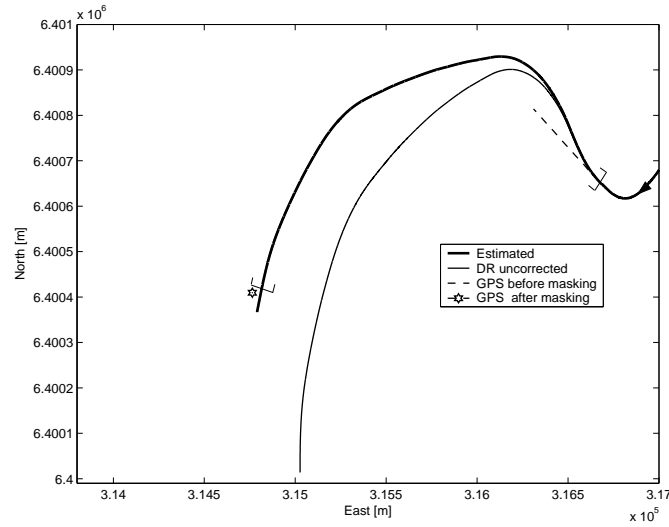


Figure 6.13. The GPS trajectory (before and after signal masking), the estimated trajectory and the DR trajectory performed with raw measurements (DR uncorrected) through the tunnel in route 2. The brackets indicate the beginning and the end of the tunnel and the arrow indicates the direction of travel.

ure 6.12, the system had 300 seconds transient time before the GPS signal masking occurred. A longer transient time will probably give better positioning system performance, because a longer transient time will lead to better filter estimates. These estimates are, as mentioned in Section 6.3, used to correct the raw measurements during GPS signal masking. The better these corrections are, the better accuracy of the estimated trajectory. If the road turns sharply at the same time as the GPS data is lost, the positioning system performance during GPS signal masking will be affected in a negative way. This is because the GPS receiver will estimate the direction of travel to be straight ahead during GPS signal masking and as mentioned in Section 6.3, two incorrect estimated GPS positions will therefore be used in the Kalman filter before GPS signal masking is detected. This will of course have a negative affect on the quality of the estimates. This problem could be avoided if the third latest estimate of the offsets and the speed scale factor were saved and used to correct the measurements of the attitude velocities and the speed when GPS signal masking occurs. A lot of turns just before GPS signal masking will also affect the performance in a negative way, due to the fact that the filter estimates are negatively affected by a high yaw rate.

Chapter 7

Positioning System with Error State Model

In this thesis, the proposed approach to integrate DR and GPS is the complete vehicle state model approach. Another integration approach described in Section 3.4 is the error state model approach. In this chapter, a positioning system with an error state model is presented. In order to derive the error state model, the errors in the DR and the GPS has to be modelled.

7.1 Error state equations

In order to model the errors in the DR, the DR equations for position and attitude updates can be investigated. These nonlinear equations are, as described in Section 3.1,

$$\begin{aligned}N(k+1) &= N(k) + v(k)T\cos(\Theta(k))\cos(\Psi(k)) \\E(k+1) &= E(k) + v(k)T\cos(\Theta(k))\sin(\Psi(k)) \\Z(k+1) &= Z(k) + v(k)T\sin(\Theta(k)) \\ \Psi(k+1) &= \Psi(k) + T\dot{\Psi}(k) \\ \Theta(k+1) &= \Theta(k) + T\dot{\Theta}(k)\end{aligned}$$

These equations can be approximated with first order Taylor expansions, as described in Section 4.4. If the DR trajectory is chosen as the nominal trajectory,

the linearised equations about the DR trajectory can be written as

$$\delta N(k+1) = \delta N(k) + T \cos(\Theta(k)) \cos(\Psi(k)) \delta v(k) \quad (7.1)$$

$$\begin{aligned} & - v(k) T \sin(\Theta(k)) \cos(\Psi(k)) \delta \Theta(k) \\ & - v(k) T \cos(\Theta(k)) \sin(\Psi(k)) \delta \Psi(k) \end{aligned}$$

$$\delta E(k+1) = \delta E(k) + T \cos(\Theta(k)) \sin(\Psi(k)) \delta v(k) \quad (7.2)$$

$$\begin{aligned} & - v(k) T \sin(\Theta(k)) \sin(\Psi(k)) \delta \Theta(k) \\ & + v(k) T \cos(\Theta(k)) \cos(\Psi(k)) \delta \Psi(k) \end{aligned}$$

$$\delta Z(k+1) = \delta Z(k) + T \sin(\Theta(k)) \delta v(k) + v(k) T \cos(\Theta(k)) \delta \Theta(k) \quad (7.3)$$

$$\delta \Psi(k+1) = \delta \Psi(k) + T \delta \dot{\Psi}(k) \quad (7.4)$$

$$\delta \Theta(k+1) = \delta \Theta(k) + T \delta \dot{\Theta}(k) \quad (7.5)$$

The δ :s in these equations are indicating the error in the corresponding parameter, for example, δN is the error in the north coordinate. These errors are called system errors.

The expressions (7.1)–(7.5) describe how the system errors propagate in the DR and are a linear DR error model. In order to complete the DR error model, the error in measured speed (δv), the error in measured yaw rate ($\delta \Psi$) and the error in measured pitch rate ($\delta \Theta$) have to be modelled. These errors are referred to as in-vehicle sensor errors and are modelled as in Section 6.1, with the distinction that all speedometer errors are modelled as white Gaussian noise.

The errors in the GPS have to be modelled as well to complete the error state model. The GPS errors are modelled, as in Section 6.1, as measurement noise.

7.2 Implementation of the error state model

The positioning system with a system error state model has been implemented in Simulink and a system overview can be seen in Figure 7.1. The GPS position is given in WGS-84 coordinates and transformed to UTM with the expressions in Appendix B.1. The DR is performed as described in the complete vehicle state approach in Section 6.3. The GPS position at time k is a delayed measurement and to make the Kalman filter equations consistent, the output from the DR block is delayed with t_{gps} .

The signal model in this approach is an error model described by (7.1)–(7.5) and (6.1)–(6.2). The state vector in the error state model is

$$x = (\delta N \ \delta E \ \delta Z \ \delta \Psi \ \delta \Theta \ \Delta_{\dot{\Psi}} \ \Delta_{\dot{\Theta}})^T$$

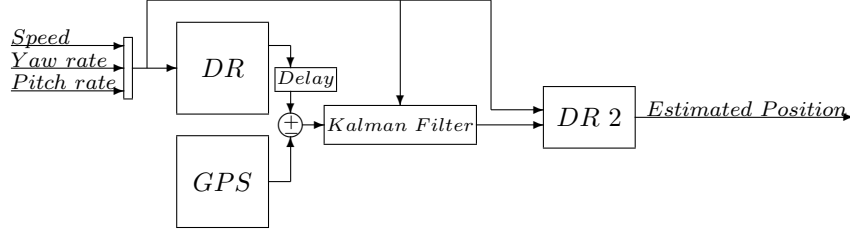


Figure 7.1. A schematic overview of the positioning system with an error state model.

The use of first order Taylor expansions in Section 7.1 implies that a linearised Kalman filter can be used. The differences between the DR and the GPS positions are used as measurements, which gives the following measurement equations

$$GPS_N(k) - DR_N(k) = \delta N(k) + e_1 \quad (7.6)$$

$$GPS_E(k) - DR_E(k) = \delta E(k) + e_2 \quad (7.7)$$

$$GPS_Z(k) - DR_Z(k) = \delta Z(k) + e_3 \quad (7.8)$$

Here GPS_N , GPS_E and GPS_Z are the GPS north, east and vertical position coordinates, respectively, and DR_N , DR_E and DR_Z are the corresponding DR coordinates.

In the linearised Kalman filter equations, F , G and H matrices are needed. These matrices can be found in Appendix A.3 and are defined as in Section 4.4. Since the parameters in the F matrix depend on the time-varying variables speed, yaw angle and pitch angle, a time varying linearised Kalman filter has to be used. The Q and R matrices are in this thesis considered as design parameters. However, to get a starting point in the design process, the Q matrix is approximated with the uncertainties in (7.1)–(7.5) and (6.1)–(6.2). To get the starting values for the R matrix the uncertainties in (7.6)–(7.8) are used as the diagonal elements in the R matrix.

The Kalman filter estimates correct the output from the first DR block, i.e. the estimated errors in N , E and Z are used to correct the position and the estimated errors in the attitude are used to correct the attitude. To be able to use the estimates as corrections in the DR, a second DR block has to be introduced. If the estimated errors would be fed back to the first DR block, remaining errors will always be present. This is due to the fact that the Kalman filter needs a difference between the measurement and the true value to estimate a present error. This can be made clear by considering the yaw rate offset. If the measured

yaw rate should be corrected equal to the true yaw rate, i.e. the yaw rate offset is equal to zero, the DR position will not drift from the true position. When there is no drift in the DR position, the next Kalman filter offset estimate will be zero. When this estimate is used as a correction in the DR, no correction is made to the measured yaw rate, which still has an offset needed to be compensated for. This is the reason why an error in a feedback solution cannot be totally compensated for.

The second DR block is restarted with corrected position and attitude from the first DR block. In between two Kalman filter updates, DR is performed in the second DR block with measured speed and measured angular velocities, corrected with the latest Kalman filter offset estimates. The output from the second DR is the system output and can be delivered in both WGS-84 coordinates and UTM coordinates.

7.3 Evaluation of positioning system with error state model

The evaluation of the positioning system with the error state model shows that this approach is not able to give a correct estimated position or attitude. The major problem for the error state model is the large offset of the gyroscope used in this thesis.

The evaluation of the positioning system with an error state model has been done with data constructed from the measurements of speed and yaw rate. The pitch rate is assumed to be zero in this evaluation. The constructed data can be considered as true measurements, i.e. measurements free from sensor errors. To evaluate the ability of the positioning system to handle a specific sensor error, sensor errors can be added to the constructed data. Sensor error free data are constructed by considering the measurements of the speed and yaw rate to be the true speed and yaw rate. These signals are then used to calculate a trajectory and from this trajectory GPS data can be created. By taking a position every other second from this trajectory, perfect GPS signals are constructed as shown in Figure 7.2. The speed and yaw rate measurements used to create the perfect GPS signals, are the signals used in the DR in the evaluation. The Q , R and P_0 matrices that have been used in this evaluation can be found in Appendix A.4.

When an offset of $3 \cdot 10^{-3}$ rad/s, which is approximately the offset of the used gyroscope signal is added to the yaw rate signal the positioning system is unable to estimate a correct position. This is due to the fact that the yaw rate offset implies that the error in yaw angle in the first DR block grows too large with time. Hence, the assumption of small errors made in the derivation of the error propagation in the DR is not fulfilled, i.e. the linearisation around the DR trajectory becomes invalid. After 1000 s, the error in the yaw angle is nearly 180° and cannot be considered a small error. Because of this large error, the Kalman filter is unable

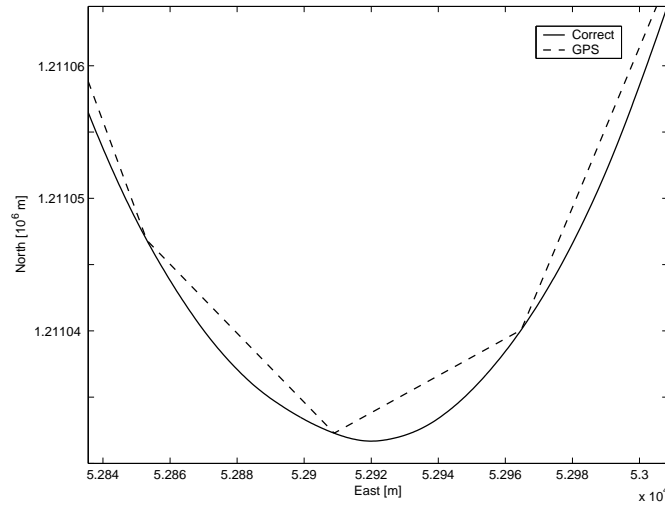


Figure 7.2. The GPS position is created from a trajectory calculated with signals considered to be error free. By taking a position from this trajectory every other second, GPS positions are created.

to estimate the right corrections of the position. After 1000 s the estimated position differs 100 m in the north coordinate and 80 m in the east coordinate from the true values and these errors will increase with time. This can be seen in Figure 7.3.

The error state model approach can be a correct approach to use if the gyroscope has an extremely low offset or if the operation time is short. This approach has successfully been used in [14], where the gyroscope offset is $2 \cdot 10^{-8}$ rad/s. However, the gyroscope used in this thesis has too large offset for the error state model approach to work satisfactory. The positioning system with complete vehicle state model that is presented in Chapter 6 is, for the sensors used in this thesis, proven to be superior.

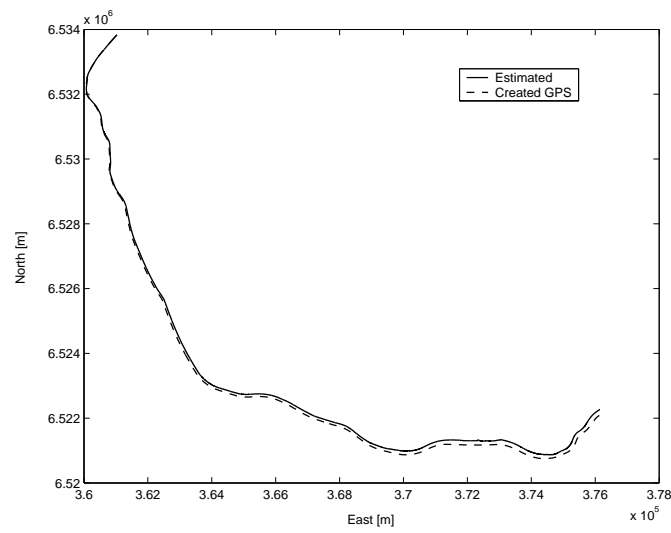


Figure 7.3. The estimated trajectory from the positioning system with error state model and the created GPS trajectory, i.e. the trajectory considered to be true. After 1000 s the estimated position differs 100 m in the north coordinate and 80 m in the east coordinate from the true values and these errors will increase with time.

Chapter 8

Map Matching

In order to increase the accuracy of the positioning system with a complete vehicle state model in Chapter 6, a map matching algorithm has been added to the system. In this chapter, implementation and evaluation of a probabilistic point-to-point and heading map matching algorithm is presented.

8.1 Map data base

In order to perform map matching, a map data base, is needed. In the map data base shape points of the road network are stored. In this thesis the information stored in the shape points are the N and E coordinates and the direction of travel. The information has been collected using the positioning system from Chapter 6. The shape points are stored with about 3 m intervals.

8.2 Implementation of a probabilistic point-to-point and heading map matching algorithm

A probabilistic point-to-point and heading map matching algorithm has been implemented in Simulink. The input to the map matching algorithm has been the estimated trajectory from the positioning system in Chapter 6. The map matching is only done in the north-east plane. As discussed in Section 3.5, Kalman filter estimated positions are very convenient to use in map matching. This is because an approximation of the covariance matrix of the estimate errors, the P matrix, is available from the EKF. This P matrix can be used to define the confidence regions of the estimates. In this thesis, only the diagonal elements in the P matrix are used. By taking the square root of these diagonal elements, an approximation of the standard deviations (σ) for the estimates are derived. The N and E standard deviations are multiplied with a factor C_A and the heading standard deviation with a factor C_B . These factors allow the user to adjust the size of the confidence region.

In order to make the search algorithms easy to implement, the confidence region for the position is given a squared shape. This is done by defining a square around the estimated position with the base $2C_A\sigma_E$ and the height $2C_A\sigma_N$.

In order to use a confidence region, the confidence level has to be specified. Unfortunately, it is difficult to determine the confidence level for the square shaped confidence region mentioned above. This is because the distribution of the estimated position is difficult to determine and that the P matrix from the EKF is just an approximation of the covariance matrix of the estimate errors. However, the confidence regions will approximately have the same confidence level from one sample to another.

The first step for the map matching algorithm is to search the map data base for shape points within the confidence region. In this thesis, the search algorithm compares all the shape points in the map data base with the confidence region. In order to get a functional on-line algorithm, this search algorithm has to be improved. The shape points that are within the confidence region are chosen by the search algorithm and stored for further evaluation. The evaluation equation is described by

$$V = |Pos_e - Pos_m| + C_C|\Psi_e - \Psi_m| \quad (8.1)$$

where Pos_e is the estimated position coordinates, Pos_m is the stored position coordinates of the shape points, Ψ_e is the estimated yaw angle, Ψ_m is the stored direction of travel at the shape points and C_C is a design parameter. The stored shape point with the smallest V value is said to be the position the estimated position is matched to. If there are no shape points in the map data base that lies in the confidence region, the estimated position itself is chosen as the output.

8.3 Evaluation of the map matching algorithm

The map matching system described above has been evaluated with respect to three different cases, which are presented below. The system has only been implemented as an off-line solution. Therefore, it has not been evaluated if it is possible to process the integration of the map matching system and the EKF with a frequency of 50 Hz. The design parameters C_A , C_B and C_C have been adjusted in order to make the map matching system work properly for the three cases studied. To get optimal parameters, more design work still needs to be done. In this study, C_A and C_B were set to 3 and C_C was set to 100. The map matching is performed every other second and the estimated position from the positioning system is provided with 50 Hz.

The first case studied is a curve and as can be seen in Figure 8.1, the map matching algorithm is able to match the estimated position to the correct shape points. The reason why there are shape points to which no estimated position is matched, is that the map matching is performed only every other second.

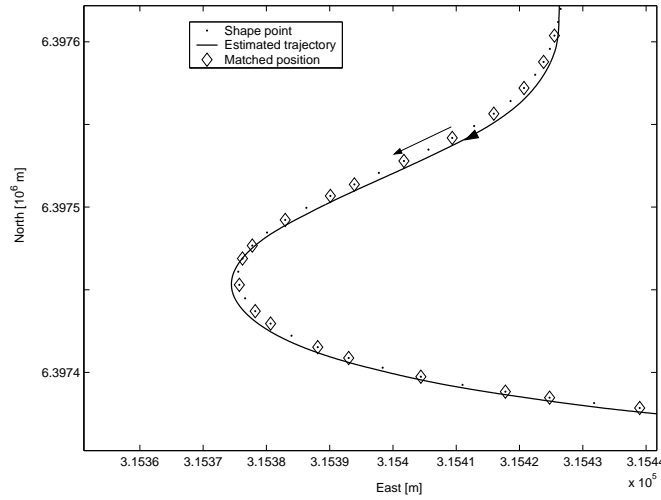


Figure 8.1. The estimated trajectory is matched to the shape points. The arrows indicate the direction of travel of the estimated trajectory and the direction of the road in the map data base.

In the second case, there are two parallel roads close to each other, but with opposite direction of travel. As can be seen in Figure 8.2, the estimated trajectory is closer to the road with the opposite direction of travel. Despite this, the estimated trajectory should of course be matched to the shape points with the same direction of travel as the estimated position and not to the closest shape points. As can be seen in Figure 8.2, the probabilistic point-to-point and heading map matching algorithm seems to handle this case with a satisfactory result. The closest shape points have opposite direction of travel and are therefore excluded from the evaluation phase where (8.1) is calculated.

The third case studied is a case where the vehicle is driving off-road. An example of off-road driving is when the vehicle is driving on a road not represented in the map data base. This is illustrated in Figure 8.3, where the estimated trajectory itself is chosen as the output, as soon as no shape point is within the confidence region. This can be seen in the middle of the figure, where the road stored in the map data base turns to the right, but the vehicle continues to travel straight ahead on a road which is not represented with shape points in the map data base.

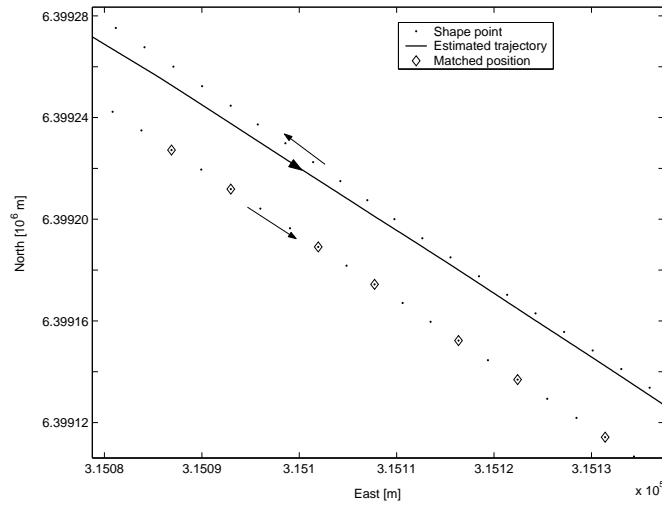


Figure 8.2. The estimated trajectory is matched to the lower of the two roads even though it is closer to the road above. This is because the direction of travel is considered in the map matching algorithm. The arrows indicate the direction of the estimated trajectory and the directions of the two roads in the map data base.

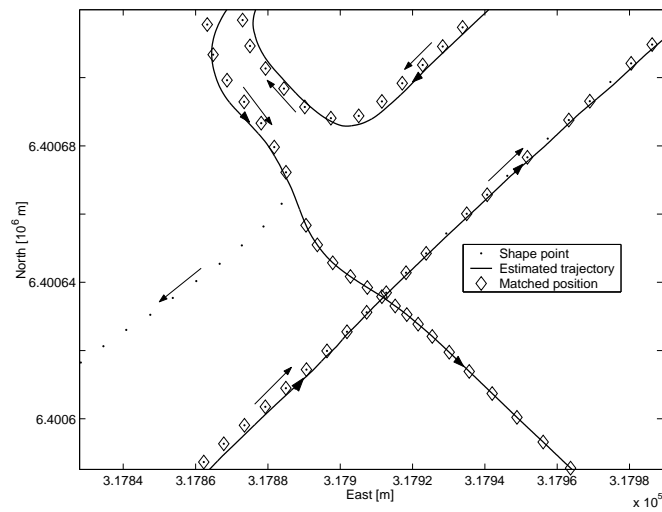


Figure 8.3. The estimated trajectory is not matched to any shape point when no shape point is within the confidence region. This gives good position accuracy when the vehicle is driving off-road. The arrows indicate the direction of the estimated trajectory and the directions of the roads in the map data base.

Chapter 9

Conclusions

In this chapter, the results of the evaluation of the positioning system with a complete vehicle state model and the evaluation of the positioning system with an error state model, are summarized. The results of the map matching evaluation and some ideas for future work are also presented in this chapter.

9.1 Results

The evaluation shows that the positioning system with a complete vehicle state model is able to give an estimated position in the horizontal plane with a relatively high update frequency. After the transient time of the Kalman filter, the estimated position has the same accuracy as the GPS receiver used. Furthermore, it is shown that the system can handle GPS signal masking for a period of time. For example, after a 2060 m long tunnel, where GPS signal masking has occurred, the estimated position differs about 25 m in north and east coordinates compared to the GPS position after the tunnel. This result is satisfactory and therefore the complete vehicle state model is considered to be a proper approach to use in similar conditions as in this thesis. The positioning system with a complete vehicle state model does not estimate the pitch angle satisfactory. This results in a growing error with time in the height component during GPS signal masking. In order to investigate if whether better estimates of the pitch angle and the height component can be obtained, more design and evaluation work have to be done.

The evaluation of the positioning system with an error state model shows that this approach is not suitable for sensor errors as large as in this thesis. The error in the estimated position will grow large with time in this approach, due to the large gyroscope offset.

The implemented map matching algorithm is a probabilistic algorithm. The evaluation shows that the algorithm is able to distinguish roads with different directions

of travel from each other and also that it is able to handle off-road driving.

9.2 Future work

To improve the performance of the positioning system, more development work has to be done. To use the third latest estimates of the offsets and the speed scale factor during GPS signal masking, is one example of an improvement that can be done. This should be done due to the fact that it takes two GPS measurements before GPS signal masking is detected. These two GPS measurements affect the filter estimates in a negative way and this leads to a decreased system performance during GPS signal masking. Another improvement that can be done is to restart the filter after GPS signal masking with the latest measurements of speed, yaw rate and pitch rate instead of the last estimates. Furthermore, it might be possible to decrease the transient time of the Kalman filter, if the estimates and the covariance matrix from the last running time are used.

Another interesting aspect to evaluate, is how the characteristics of the in-vehicle sensors and the GPS receiver effect the system performance. The use of a GPS receiver that provides the time delay of the measured position, should probably increase the system performance. Examples of other interesting characteristics to examine are the GPS update frequency, the magnitude of the gyroscope offset and the resolution of the gyroscope. In order to determine the quality of the pitch angle estimate, more evaluation work has to be done.

Two important improvements of the map matching algorithm that can be done, are to develop the search algorithm and to use maps with higher accuracy than the ones used in this thesis. Finally, the use of the difference between the estimated position from the positioning system and the matched position in the Kalman filter is another way to increase the positioning system performance.

Bibliography

- [1] D. Bernstein and Kornhauser A. An introduction to map matching for personal navigation assistance. Technical report, New Jersey TIDE Center, Princeton University, August 1996.
- [2] H. Bohlin. Integrationsmetoder för tröghetsnavigeringssystem och GPS. Master's thesis LiTH-ISY-EX-1398, Department of Electrical Engineering, Linköping University, Linköping, Sweden, March 1994.
- [3] L. Zhao et al. An extended Kalman filter algorithm low cost dead reckoning system data for vehicle performance and emissions monitoring. *The Journal of Navigation*, 56:257–275, 2003.
- [4] J. Farrell and M. Barth. *The Global Positioning System & Inertial Navigation*. McGraw-Hill, New York, USA, 1998.
- [5] T. Glad and L. Ljung. *Reglerteori. Flervariabla och olinjära metoder*. Studentlitteratur, Lund, Sweden, 1st edition, 1997. In Swedish.
- [6] M. Grewal and A. Andrews. *Kalman Filtering: Theory and Practice Using MATLAB*. John Wiley & Sons, Inc, USA, 2001.
- [7] M. Grewal, L. Weill, and A. Andrews. *Global Positioning Systems, Inertial Navigation and Integration*. John Wiley & Sons, Inc, New York, USA, 2001.
- [8] P. Hall. A Bayesian approach to map-aided vehicle positioning. Master's thesis LiTH-ISY-EX-3102, Department of Electrical Engineering, Linköping University, Linköping, Sweden, January 2001.
- [9] <http://home.t-online.de/home/kontext/utm.htm>. UTM2.
- [10] <http://www.garmin.com/products/gpsmap76s/spec.html>. GPSP76S.
- [11] <http://www.tech.volvo.se>. About Volvo Technology.
- [12] T. Kailath, A.H. Sayed, and B. Hassibi. *Linear Estimation*. Prentice-Hall, Upper Saddle River, New Jersey, 2000.

- [13] J. Mei. Integrated vehicle navigation systems. Master's thesis LiTH-IDA-Ex-99/110, Department of Computer and Information Science, Linköping University, Linköping, Sweden, December 1999.
- [14] P. Nordlund. En simuleringsmiljö för tröghetsnavigering samt en metod för integration av tröghetsnavigeringssystem och GPS. Master's thesis LiTH-ISY-EX-1728, Department of Electrical Engineering, Linköping University, Linköping, Sweden, December 1996.
- [15] Y. Zhao. *Vehicle Location and Navigation System*. Artech House, Inc, Norwood, Great Britain, 1997.

Appendix A

System Matrices

This appendix contains the system matrices F , G , H and the design parameters Q , R and P_0 .

A.1 System matrices for the complete vehicle state model

The following system matrices were used in the complete vehicle state model

$$F = \begin{pmatrix} 1 & 0 & 0 & f_{14} & f_{15} & 0 & 0 & 0 & 0 & f_{110} & 0 \\ 0 & 1 & 0 & f_{24} & f_{25} & 0 & 0 & 0 & 0 & f_{210} & 0 \\ 0 & 0 & 1 & 0 & f_{35} & 0 & 0 & 0 & 0 & f_{310} & 0 \\ 0 & 0 & 0 & 1 & 0 & T & 0 & 0 & 0 & 0 & 0 \\ 0 & 0 & 0 & 0 & 1 & 0 & T & 0 & 0 & 0 & 0 \\ 0 & 0 & 0 & 0 & 0 & 1 & 0 & 0 & 0 & 0 & 0 \\ 0 & 0 & 0 & 0 & 0 & 0 & 1 & 0 & 0 & 0 & 0 \\ 0 & 0 & 0 & 0 & 0 & 0 & 0 & 1 & 0 & 0 & 0 \\ 0 & 0 & 0 & 0 & 0 & 0 & 0 & 0 & 1 & 0 & 0 \\ 0 & 0 & 0 & 0 & 0 & 0 & 0 & 0 & 0 & 1 & 0 \\ 0 & 0 & 0 & 0 & 0 & 0 & 0 & 0 & 0 & 0 & 1 \end{pmatrix}$$

$$\begin{aligned} f_{14} &= -v(k)T \cos(\Theta(k)) \sin(\Psi(k)) \\ f_{24} &= v(k)T \cos(\Theta(k)) \cos(\Psi(k)) \\ f_{15} &= -v(k)T \sin(\Theta(k)) \cos(\Psi(k)) \\ f_{25} &= -v(k)T \sin(\Theta(k)) \sin(\Psi(k)) \\ f_{35} &= v(k)T \cos(\Theta(k)) \\ f_{110} &= T \cos(\Theta(k)) \cos(\Psi(k)) \\ f_{210} &= T \cos(\Theta(k)) \sin(\Psi(k)) \\ f_{310} &= T \sin(\Theta(k)) \end{aligned}$$

[illegible]

[illegible]

A.2 Design matrices for the complete vehicle state model

In the evaluation of the complete vehicle state approach, the following values of the Q , R and P_0 matrices were used

$$Q = \begin{pmatrix} 10^{-5} & 0 & 0 & 0 & 0 & 0 & 0 & 0 & 0 & 0 & 0 \\ 0 & 10^{-5} & 0 & 0 & 0 & 0 & 0 & 0 & 0 & 0 & 0 \\ 0 & 0 & 10^{-5} & 0 & 0 & 0 & 0 & 0 & 0 & 0 & 0 \\ 0 & 0 & 0 & 10^{-2} & 0 & 0 & 0 & 0 & 0 & 0 & 0 \\ 0 & 0 & 0 & 0 & 10^{-2} & 0 & 0 & 0 & 0 & 0 & 0 \\ 0 & 0 & 0 & 0 & 0 & 10^{-1} & 0 & 0 & 0 & 0 & 0 \\ 0 & 0 & 0 & 0 & 0 & 0 & 10^{-1} & 0 & 0 & 0 & 0 \\ 0 & 0 & 0 & 0 & 0 & 0 & 0 & 10^{-7} & 0 & 0 & 0 \\ 0 & 0 & 0 & 0 & 0 & 0 & 0 & 0 & 10^{-7} & 0 & 0 \\ 0 & 0 & 0 & 0 & 0 & 0 & 0 & 0 & 0 & 10^0 & 0 \\ 0 & 0 & 0 & 0 & 0 & 0 & 0 & 0 & 0 & 0 & 10^{-5} \end{pmatrix}$$

$$R = \begin{pmatrix} 5 \cdot 10^1 \cdot DOP & 0 & 0 & 0 & 0 & 0 & 0 & 0 \\ 0 & 5 \cdot 10^1 \cdot DOP & 0 & 0 & 0 & 0 & 0 & 0 \\ 0 & 0 & 2 \cdot 10^2 \cdot DOP & 0 & 0 & 0 & 0 & 0 \\ 0 & 0 & 0 & 10^{-2} & 0 & 0 & 0 & 0 \\ 0 & 0 & 0 & 0 & 10^{-2} & 0 & 0 & 0 \\ 0 & 0 & 0 & 0 & 0 & 10^{12} & 0 & 0 \\ 0 & 0 & 0 & 0 & 0 & 0 & 10^{-2} & 0 \end{pmatrix}^2$$

$$P_0 = 50 \cdot \begin{pmatrix} 10^2 & 0 & 0 & 0 & 0 & 0 & 0 & 0 & 0 & 0 & 0 \\ 0 & 10^2 & 0 & 0 & 0 & 0 & 0 & 0 & 0 & 0 & 0 \\ 0 & 0 & 2 \cdot 10^3 & 0 & 0 & 0 & 0 & 0 & 0 & 0 & 0 \\ 0 & 0 & 0 & (\frac{\pi}{180})^2 & 0 & 0 & 0 & 0 & 0 & 0 & 0 \\ 0 & 0 & 0 & 0 & (\frac{\pi}{180})^2 & 0 & 0 & 0 & 0 & 0 & 0 \\ 0 & 0 & 0 & 0 & 0 & 10^1 & 0 & 0 & 0 & 0 & 0 \\ 0 & 0 & 0 & 0 & 0 & 0 & 10^1 & 0 & 0 & 0 & 0 \\ 0 & 0 & 0 & 0 & 0 & 0 & 0 & 4 \cdot 10^{-6} & 0 & 0 & 0 \\ 0 & 0 & 0 & 0 & 0 & 0 & 0 & 0 & 4 \cdot 10^{-6} & 0 & 0 \\ 0 & 0 & 0 & 0 & 0 & 0 & 0 & 0 & 0 & 2 & 0 \\ 0 & 0 & 0 & 0 & 0 & 0 & 0 & 0 & 0 & 0 & 10^{-2} \end{pmatrix}$$

A.3 System matrices for the error state model

The following system matrices were used in the error state positioning system

$$F = \begin{pmatrix} 1 & 0 & 0 & f_{14} & f_{15} & 0 & 0 \\ 0 & 1 & 0 & f_{24} & f_{25} & 0 & 0 \\ 0 & 0 & 1 & 0 & f_{35} & 0 & 0 \\ 0 & 0 & 0 & 1 & 0 & T & 0 \\ 0 & 0 & 0 & 0 & 1 & 0 & T \\ 0 & 0 & 0 & 0 & 0 & 1 & 0 \\ 0 & 0 & 0 & 0 & 0 & 0 & 1 \end{pmatrix}$$

where

$$\begin{aligned} f_{14} &= -v(k)T\cos(\Theta(k))\sin(\Psi(k)) \\ f_{24} &= v(k)T\cos(\Theta(k))\cos(\Psi(k)) \\ f_{15} &= -v(k)T\sin(\Theta(k))\cos(\Psi(k)) \\ f_{25} &= -v(k)T\sin(\Theta(k))\sin(\Psi(k)) \\ f_{35} &= v(k)T\cos(\Theta(k)) \end{aligned}$$

$$G = \begin{pmatrix} g_{11} & 0 & 0 & 0 & 0 & 0 & 0 \\ 0 & g_{22} & 0 & 0 & 0 & 0 & 0 \\ 0 & 0 & g_{33} & 0 & 0 & 0 & 0 \\ 0 & 0 & 0 & T & 0 & 0 & 0 \\ 0 & 0 & 0 & 0 & T & 0 & 0 \\ 0 & 0 & 0 & 0 & 0 & 1 & 0 \\ 0 & 0 & 0 & 0 & 0 & 0 & 1 \end{pmatrix}$$

where

$$\begin{aligned} g_{11} &= T\cos(\Theta(k))\cos(\Psi(k)) \\ g_{22} &= T\cos(\Theta(k))\sin(\Psi(k)) \\ g_{33} &= T\sin(\Theta(k)) \end{aligned}$$

$$H = \begin{pmatrix} 1 & 0 & 0 & 0 & 0 & 0 & 0 \\ 0 & 1 & 0 & 0 & 0 & 0 & 0 \\ 0 & 0 & 1 & 0 & 0 & 0 & 0 \\ 0 & 0 & 0 & 1 & 0 & 0 & 0 \end{pmatrix}$$

A.4 Design parameters for the error state model

In the error state model approach, the following Q , R and P_0 matrices were used in the evaluation of the error state model

$$Q = \begin{pmatrix} 10^{-3} & 0 & 0 & 0 & 0 & 0 & 0 \\ 0 & 10^{-3} & 0 & 0 & 0 & 0 & 0 \\ 0 & 0 & 10^{-3} & 0 & 0 & 0 & 0 \\ 0 & 0 & 0 & 10^{-4} & 0 & 0 & 0 \\ 0 & 0 & 0 & 0 & 10^{-4} & 0 & 0 \\ 0 & 0 & 0 & 0 & 0 & 4 \cdot 10^{-4} & 0 \\ 0 & 0 & 0 & 0 & 0 & 0 & 4 \cdot 10^{-4} \end{pmatrix}$$

$$R = DOP^2 \begin{pmatrix} 10 & 0 & 0 \\ 0 & 10 & 0 \\ 0 & 0 & 20 \end{pmatrix}^2$$

$$P_0 = \begin{pmatrix} 10 & 0 & 0 & 0 & 0 & 0 & 0 \\ 0 & 10 & 0 & 0 & 0 & 0 & 0 \\ 0 & 0 & 40 & 0 & 0 & 0 & 0 \\ 0 & 0 & 0 & \left(\frac{5\cdot\pi}{180}\right)^2 & 0 & 0 & 0 \\ 0 & 0 & 0 & 0 & \left(\frac{5\cdot\pi}{180}\right)^2 & 0 & 0 \\ 0 & 0 & 0 & 0 & 0 & 10^{-5} & 0 \\ 0 & 0 & 0 & 0 & 0 & 0 & 10^{-5} \end{pmatrix}$$

Appendix B

Transformations

In this appendix, the transformations between WGS-84 coordinates and UTM coordinates, and vice versa, are given.

B.1 Transformation between WGS-84 and UTM coordinates

Transformation between WGS-84 coordinates, latitude(ϕ) and longitude (λ), and conformal UTM coordinates, east (E) and north (N), are given by the following series expansion

$$\begin{aligned} N = & kS(\phi) + kN\left(\frac{t}{2}\cos^2\phi(\lambda - \lambda_0)^2 + \frac{t}{24}\cos^4\phi(5 - t^2 + 9\eta^2 + 4\eta^4)(\lambda - \lambda_0)^4\right. \\ & + \frac{t}{720}\cos^6\phi(61 - 58t^2 + t^4 + 270\eta^2 - 330t^2\eta^2)(\lambda - \lambda_0)^6 \\ & \left. + \frac{t}{40320}\cos^8\phi(1385 - 3111t^2 + 543t^4 - t^6)(\lambda - \lambda_0)^8 + \dots\right) \end{aligned}$$

$$\begin{aligned} E = & kN(\cos\phi(\lambda - \lambda_0) + \frac{1}{6}\cos^3\phi(1 - t^2 + \eta^2)(\lambda - \lambda_0)^3 \\ & + \frac{1}{120}\cos^5\phi(5 - 18t^2 + t^4 + 14\eta^2 - 58t^2\eta^2)(\lambda - \lambda_0)^5 \\ & + \frac{1}{5040}\cos^7\phi(61 - 479t^2 + 179t^4 - t^6)(\lambda - \lambda_0)^7 + \dots) \end{aligned}$$

where

$$S(\phi) = \text{Arc length of meridian} = \alpha [\phi + \beta \sin 2\phi + \gamma \sin 4\phi + \delta \sin 6\phi + \epsilon \sin 8\phi + \dots]$$

$$\alpha = 6367449.1458 \text{ m}$$

$$\beta = -2.51882792 \cdot 10^{-3}$$

$$\gamma = 2.64354 \cdot 10^{-6}$$

$$\delta = -3.45 \cdot 10^{-9}$$

$$\epsilon = 5 \cdot 10^{-12}$$

$$N = \text{Radius of curvature in prime vertical} = \frac{a^2}{b\sqrt{1 + \eta^2}}$$

$$\eta^2 = \text{Auxiliary quantity} = \epsilon^2 \cos^2 \phi$$

$$\epsilon^2 = \text{Second numerical eccentricity} = \frac{a^2 - b^2}{b^2}$$

$$t = \text{Auxiliary quantity} = \tan \phi$$

$$\lambda_0 = \text{Longitude of central meridian}$$

$$k = \text{UTM scale factor} = 0.9996$$

$$a = \text{Semi-major axis} = 6378137 \text{ m}$$

$$b = \text{Semi-minor axis} = 6356752 \text{ m}$$

B.2 Transformation between UTM and WGS-84 coordinates

The inverse UTM projection, transformation between a point (N, E) on the UTM-plane to a point (ϕ , λ) on the WGS-84 ellipsoid is given by the following series

expansion

$$\begin{aligned}
\phi &= \phi_f - \frac{t_f}{2}(1 + \eta_f^2) \left(\frac{x}{kN_f} \right)^2 \\
&+ \frac{t_f}{24}(5 + 3t_f^2 + 6\eta_f^2 - 6t_f^2\eta_f^2 - 3\eta_f^4 - 9t_f^2\eta_f^4) \left(\frac{x}{kN_f} \right)^4 \\
&- \frac{t_f}{720}(61 + 90t_f^2 + 45t_f^4 + 107\eta_f^2 - 162t_f^2\eta_f^2 - 45t_f^4\eta_f^2) \left(\frac{x}{kN_f} \right)^6 \\
&+ \frac{t_f}{40320}(1385 + 3633t_f^2 + 4095t_f^4 + t_f^6) \left(\frac{x}{kN_f} \right)^8 + \dots \\
\\
\lambda &= \lambda_0 + \frac{1}{\cos\phi_f} \left(\frac{x}{kN_f} \right) - \frac{1}{6\cos\phi_f}(1 + 2t_f^2 + \eta_f^2) \left(\frac{x}{kN_f} \right)^3 \\
&+ \frac{1}{120\cos\phi_f}(5 + 28t_f^2 + 24t_f^4 + 6\eta_f^2 + 8t_f^2\eta_f^2) \left(\frac{x}{kN_f} \right)^5 \\
&- \frac{1}{5401\cos\phi_f}(61 + 662t_f^2 + 1320t_f^4 + 720t_f^6) \left(\frac{x}{kN_f} \right)^7 + \dots
\end{aligned}$$

where the terms with the subscript f must be computed based on the footpoint latitude ϕ_f , which is given by the following series expansion

$$\phi_f = \frac{y}{k\bar{\alpha}} + \bar{\beta}\sin 2\frac{y}{k\bar{\alpha}} + \bar{\gamma}\sin 4\frac{y}{k\bar{\alpha}} + \bar{\delta}\sin 6\frac{y}{k\bar{\alpha}} + \bar{\epsilon}\sin 8\frac{y}{k\bar{\alpha}} + \dots$$

where

$$\begin{aligned}
\bar{\alpha} &= 6367449.1458 \text{ m} \\
\bar{\beta} &= 2.51882658 \cdot 10^{-3} \\
\bar{\gamma} &= 3.70095 \cdot 10^{-6} \\
\bar{\delta} &= 7.45 \cdot 10^{-9} \\
\bar{\epsilon} &= 17 \cdot 10^{-12}
\end{aligned}$$

På svenska

Detta dokument hålls tillgängligt på Internet – eller dess framtida ersättare – under en längre tid från publiceringsdatum under förutsättning att inga extraordinära omständigheter uppstår.

Tillgång till dokumentet innebär tillstånd för var och en att läsa, ladda ner, skriva ut enstaka kopior för enskilt bruk och att använda det oförändrat för ickekommersiell forskning och för undervisning. Överföring av upphovsrätten vid en senare tidpunkt kan inte upphäva detta tillstånd. All annan användning av dokumentet kräver upphovsmannens medgivande. För att garantera äktheten, säkerheten och tillgängligheten finns det lösningar av teknisk och administrativ art.

Upphovsmannens ideella rätt innefattar rätt att bli nämnd som upphovsman i den omfattning som god sed kräver vid användning av dokumentet på ovan beskrivna sätt samt skydd mot att dokumentet ändras eller presenteras i sådan form eller i sådant sammanhang som är kränkande för upphovsmannens litterära eller konstnärliga anseende eller egenart.

För ytterligare information om Linköping University Electronic Press se förlagets hemsida <http://www.ep.liu.se/>

In English

The publishers will keep this document online on the Internet - or its possible replacement - for a considerable time from the date of publication barring exceptional circumstances.

The online availability of the document implies a permanent permission for anyone to read, to download, to print out single copies for your own use and to use it unchanged for any non-commercial research and educational purpose. Subsequent transfers of copyright cannot revoke this permission. All other uses of the document are conditional on the consent of the copyright owner. The publisher has taken technical and administrative measures to assure authenticity, security and accessibility.

According to intellectual property law the author has the right to be mentioned when his/her work is accessed as described above and to be protected against infringement.

For additional information about the Linköping University Electronic Press and its procedures for publication and for assurance of document integrity, please refer to its WWW home page: <http://www.ep.liu.se/>

© [David Andersson, Johan Fjellström]